Coordination Chemistry Reviews 254 (2010) 1726–1747

Contents lists available at ScienceDirect

Coordination Chemistry Reviews

journal homepage: www.elsevier.com/locate/ccr

Review

Recognition of anions by polyammonium macrocyclic and cryptand receptors: Influence of the dimensionality on the binding behavior

Pedro Mateus[a], Nicolas Bernier[a], Rita Delgado[a,b,*]

[a] Instituto de Tecnologia Química e Biológica, Universidade Nova de Lisboa, Av. da República - EAN, 2780-157 Oeiras, Portugal
[b] Instituto Superior Técnico, DEQB, Av. Rovisco Pais, 1049-001 Lisboa, Portugal

Contents

ARTICLE INFO

Article history:
Received 27 July 2009
Accepted 4 November 2009
Available online 12 November 2009

Keywords:
Macrocycle
Cryptand
Anion
Substrate
Receptor
Association constants
Effective constant

ABSTRACT

Seven pairs of macrocyclic/cryptand polyamines, differing only in the added dimensionality, were selected and evaluated as receptors for anions in aqueous solution. The main differences on binding properties of protonated macrocycles and protonated cryptands as receptors for anions were analyzed through the association constants and structural data from the literature. Reported stepwise association constant values were critically evaluated on the basis of diagrams of log K_{eff} in function of pH, being K_{eff} the effective constant values.

© 2009 Elsevier B.V. All rights reserved.

1. Introduction

Considerable effort in achieving selective recognition of anions by artificial receptors has been undertaken by supramolecular chemists, mainly due to the potential biomedical and environmental applications that can be devised but also to the pleasure of extending the limits of knowledge and in going further on the synthesis of complex architectures [1–3]. However, the task of achieving high affinity and selectivity in aqueous medium is quite challenging not only due to the intrinsic characteristics of anions (larger sizes when compared to isoelectronic metal ions, variety of shapes, hydration energy and pH dependency), but also the difficulty of the design of the receptor, that may not be capable to confer the required rigidity and complementarity for the recognition of the partner. Furthermore the solvent itself plays a very important role in the binding process, as water is the most active competitor in the

* Corresponding author at: Instituto de Tecnologia Química e Biológica, Universidade Nova de Lisboa, Av. da República - EAN, 2780-157 Oeiras, Portugal.
Tel.: +351 214469737; fax: +351 214411277.
E-mail address: delgado@itqb.unl.pt (R. Delgado).

0010-8545/$ – see front matter © 2009 Elsevier B.V. All rights reserved.
doi:10.1016/j.ccr.2009.11.005

recognition process, strongly interacting with receptors and anions. Thus, entropy of desolvation is one of the most important terms in the overall computation of energy. The solvent also greatly affects the conformational and structural preferences of the macrocycle or cryptand and the binding modes of the receptors [4].

Polyamines are one of the most successful groups of compounds used as receptors for the binding of anions in aqueous media, due to the versatile nature of the amino group. It can be protonated to provide the necessary positive charge to interact with anions and to impart water solubility. The amino group can also act as hydrogen bond donor and as hydrogen bond acceptor if not protonated, which may be useful for the binding of protonated anions such as phosphates. Moreover many synthetic techniques are available for the formation of C–N bonds, which makes this type of compounds easily accessible. Thus amino groups have been incorporated in a variety of different topologies, from linear structures to mono- and polycyclic architectures and studied as receptors of anions [5–14].

In our group we are particularly interested in polyammonium macrocycles [15–20] and cryptands [21–23] as anion receptors, and our aim in the present review is to clarify differences of binding properties between protonated macrocycle and the corresponding protonated cryptand through a detailed analysis of reported association constants and structural data available. For this purpose we have selected, from all those reported in the literature, macrocycles and cryptands that differ from each other only in the added dimensionality, and have been studied for the same anionic substrates. To our surprise only seven pairs of polyammonium macrocycle/cryptand satisfied these criteria (see Chart 1). The selected macrocycles (**nm**, **n** = **1**. . .**7**) are designed from two diethyltriamine moieties bound by two equal chains of different spacers (or dipropyltriamine in one case, **2m**). The corresponding cryptands (**nc**) are derived from two tren moieties (or trpn) connected by three equal spacer chains.

The first drawback of this study was that, in spite of the huge number of published papers on this subject, comparisons are very difficult to establish, since most of the data were obtained under rather different conditions and with different experimental methods and, in many cases, the exact experimental conditions under which they were determined are not reported. Furthermore, the common list of anions for each pair (macrocycle/cryptand) is very scarce. The number of studied anions in each work is very limited, especially in the last decade, and the same receptor/anionic substrate system is rarely studied by different groups.

The second and most important drawback was that, while comparing association constant values, we found wrongly attributed equilibria for the stepwise constants, and the lack of reported

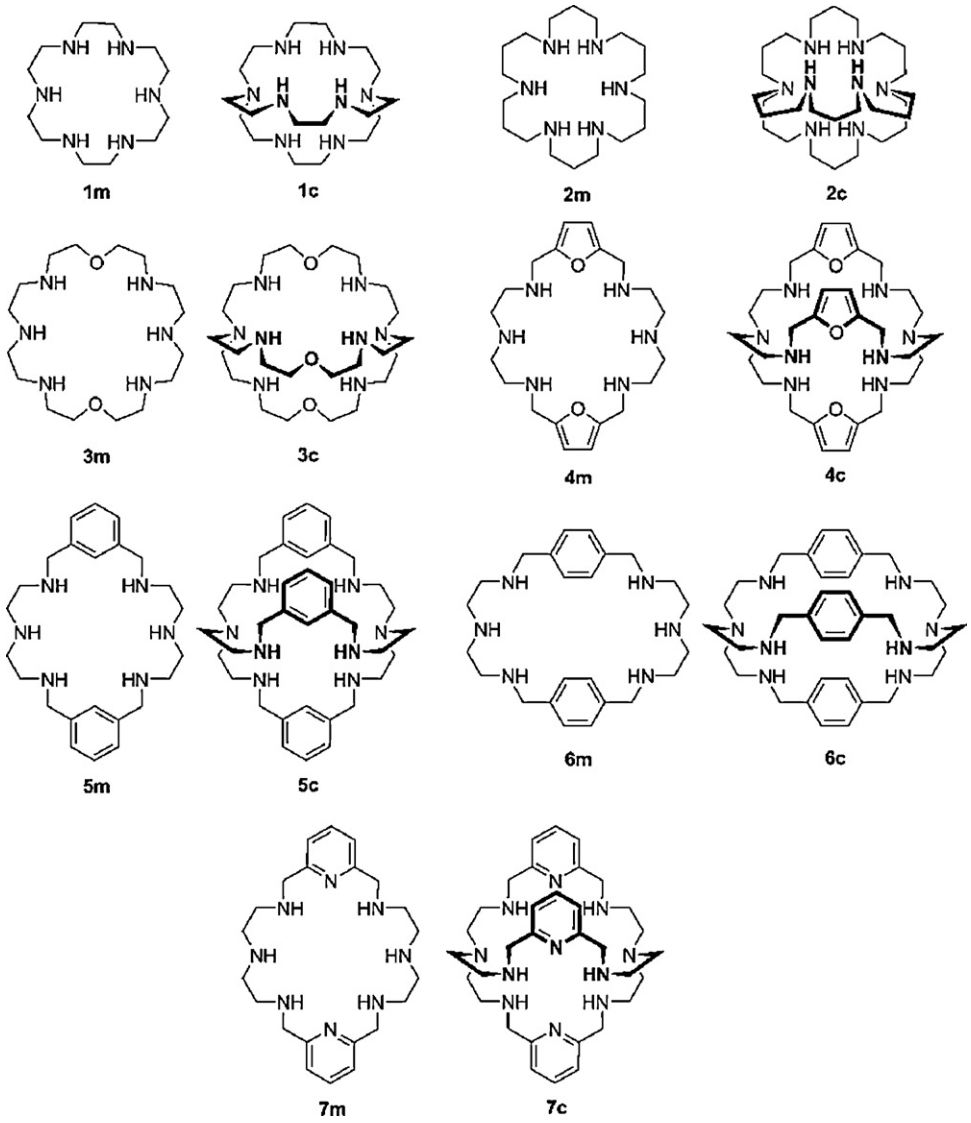

Chart 1.

Table 1
Stepwise protonation (K_i^H) constants of **1m** and **1c** in aqueous solution; T = 298.15 K.

Equilibrium	log K_i^H **1m**	$T\Delta S$, kcal mol^{-1} **1m**	ΔH, kcal mol^{-1} **1m**	log K_i^H **1c**
$L + H^+ \rightleftharpoons HL^+$	10.19[a], 10.15[b]	5.56[b]	−8.28[b]	11.18[c], 10.70[d]
$HL^+ + H^+ \rightleftharpoons H_2L^{2+}$	9.23[a], 9.48[b]	2.12[b]	−10.82[b]	9.43[c], 9.20[d]
$H_2L^{2+} + H^+ \rightleftharpoons H_3L^{3+}$	8.73[a], 8.89[b]	0.24[b]	−11.88[b]	7.59[c], 7.50[d]
$H_3L^{3+} + H^+ \rightleftharpoons H_4L^{4+}$	4.09[a], 4.24[b], 3.52[e]	−6.29[b], −9.54[e]	−12.12[b], −14.1[e]	5.78[c], 5.50[d]
$H_4L^{4+} + H^+ \rightleftharpoons H_5L^{5+}$	≈ 2[a], 2.24[b]	−0.3[b]	−3.4[b]	–
$H_5L^{5+} + H^+ \rightleftharpoons H_6L^{6+}$	≈ 1[a], 1.0[b]	–	–	–
$H_4L^{4+} + 2H^+ \rightleftharpoons H_6L^{6+}$	–	–	–	4.39[c], 5.10[d]
$L + 6H^+ \rightleftharpoons H_6L^{6+}$	35.24[a], 36.00[b]	–		38.37[c], 38.00[d]

[a] I = 0.2 M in $NaClO_4$ or NEt_4ClO_4, Ref. [27].
[b] I = 0.15 M in $NaClO_4$, Refs. [28,29].
[c] I = 0.1 M in KNO_3, Ref. [31].
[d] I = 0.1 M in Me_4NTsO, Ref. [32].
[e] I = 0.21 M in NaCl + $NaNO_3$, Ref. [30].

overall constants. This is especially pertinent for receptors and/or substrates with many and overlapping protonation states, as polyamines and polycarboxylates or polyphosphonates studied in water. Additionally, in many cases the ionic product of water, K_w, and the protonation constants of the anions are not given or not determined in the same experimental conditions. In fact the values obtained directly from fitting the experimental data using computer programs are overall (or cumulative) constants, and the stepwise constants are calculated by the authors considering certain equilibrium as the one that takes place among other possible hypothesis, and the attribution may not be the correct one. In such cases García-España and coworkers adapted the old concept derived from the coordination chemistry, the conditional constant, and by a simple extension they created the effective constant values (K_{eff}) and an easy way to check the right stepwise equilibrium. The K_{eff} values are defined as $K_{eff} = \Sigma[H_{i+j}LA]/\Sigma[H_iA] \times \Sigma[H_jL]$, where L is ligand and A the substrate [24,25]. Diagrams of K_{eff} in function of pH are helpful guides for the correct attribution of the stepwise equilibrium constant. Thus K_{eff} values are necessary in order to compare binding constants of different receptors.

To reach our aims in this review, the K_{eff} for all the studied compounds were calculated. When the overall constants are given by the authors this calculation is straightforward. When only the stepwise constants are reported, based on them and on the indicated equilibrium, we recalculated the overall constants, which together with the protonation constants of the receptor and of the anion and the K_w value, the log K_{eff} in function of pH was drawn, then the right equilibria established and the stepwise constants recalculated. Unfortunately, the present study revealed that in many systems the stepwise constant values are lower than considered by the authors, and in certain cases the differences are significant. When this happens, in the corresponding tables the reported value is followed by the recalculated value in parenthesis and with asterisk. When the table is not given due to space reasons, the log K_{eff} *versus* pH diagrams are presented.

Despite all these drawbacks, some general features derived from the dimensionality of the receptor and its effect on the binding of anions could be advanced based on the thermodynamics of the involved equilibria.

2. Protonation constants of macrocycles (1m–7m) and cryptands (1c–7c)

In polyamine systems the degree of protonation and the position of the basic centres are relevant information in order to maximize the interaction with anionic species *via* electrostatic and hydrogen-bonding interactions. Moreover, protonation affects the receptor conformation as charge repulsion causes ammonium groups to move away from each other. Thus the first aspect to analyze in order to compare polyammonium macrocycles and cryptands is their basicity and protonation behavior. An excellent review covering linear and cyclic polyamines was published [26], thus we dedicate to this subject only a short analysis centred in the chosen pairs.

In terms of the protonation behavior the macrocycle/cryptand polyamine pairs under study can be divided in two different types. The first includes pairs **1** and **2** [27–35] which consist of macrocycles and cryptands where all the amine centres are separated by the same number of carbon atoms (two for **1** and three for **2**). In the two macrocycles, **1m** and **2m**, three nitrogen atoms take three protons without much repulsion between them. As more protons are bound they will be located in amines between two already positively charged and repulsion will build up. The end result is a gap between the protonation constants of the first and the second half of nitrogen atoms, see Tables 1 and 2. For **2m** the gap is not so pronounced because the ammonium groups are separated by longer propylene chains which produce an attenuation of this grouping effect due to a lower electrostatic repulsion between positive charges.

It has been shown by NMR studies that in **1m** there is no observable charge localization in the successive first three protonation steps, due to the equivalence of the secondary amino groups [36]. This means that in solution, on the NMR time scale, the overall positive charge has a mediate homogeneous distribution over all the nitrogen atoms of the ligands.

The respective cryptands, **1c** and **2c**, have a somewhat higher overall basicity, measured by β_{H_6L} values, because the six protonable nitrogen atoms are at longer distances from each other than in the case of the corresponding macrocycles, allowing a more efficient minimization of the electrostatic repulsion between positive charges. As a consequence, the cryptands are able to be completely

Table 2
Stepwise protonation (K_i^H) constants of **2m** and **2c** in aqueous solution; T = 298.15 K.

Equilibrium	log K_i^H	
	2m[a,b]	**2c**[c]
$L + H^+ \rightleftharpoons HL^+$	10.45[a], 10.50[b]	10.45
$HL^+ + H^+ \rightleftharpoons H_2L^{2+}$	10.35[a], 10.20[b]	10.10
$H_2L^{2+} + H^+ \rightleftharpoons H_3L^{3+}$	9.05[a], 9.25[b]	9.40
$H_3L^{3+} + H^+ \rightleftharpoons H_4L^{4+}$	7.90[a], 8.00[b]	8.65
$H_4L^{4+} + H^+ \rightleftharpoons H_5L^{5+}$	7.15[a], 7.05[b]	7.00
$H_5L^{5+} + H^+ \rightleftharpoons H_6L^{6+}$	6.60[a], 6.40[b]	6.75
$H_6L^{6+} + H^+ \rightleftharpoons H_7L^{7+}$	–	4.95
$H_7L^{7+} + H^+ \rightleftharpoons H_8L^{8+}$	–	4.15
$L + 6H^+ \rightleftharpoons H_6L^{6+}$	51.50[a], 51.40[b]	52.40

[a] I = 0.1 M Me_4NCl, Ref. [33].
[b] I = 0.1 M in NaTsO, Ref. [34].
[c] I = 0.1 M in NaTsO, Ref. [35].

Table 3
Stepwise protonation (K_i^H) constants of **3m** and **3c** in aqueous solution; T = 298.15 K.

Equilibrium	$\log K_i^H$	
	3m	**3c**
$L + H^+ \rightleftharpoons HL^+$	9.15[a], 9.60[b], 9.65[c], 9.61[d]	9.99[e], 9.89[f], 9.92[g], 9.60[h]
$HL^+ + H^+ \rightleftharpoons H_2L^{2+}$	9.00[a], 9.35[b], 8.92[c], 8.89[d]	9.02[e], 9.23[f], 9.26[g], 9.35[h]
$H_2L^{2+} + H^+ \rightleftharpoons H_3L^{3+}$	8.20[a], 8.30[b], 8.30[c], 8.28[d]	7.98[e], 8.29[f], 8.22[g], 8.30[h]
$H_3L^{3+} + H^+ \rightleftharpoons H_4L^{4+}$	7.20[a], 8.10[b], 7.64[c], 7.62[d]	7.20[e], 7.65[f], 7.53[g], 7.75[h]
$H_4L^{4+} + H^+ \rightleftharpoons H_5L^{5+}$	3.70[a], 4.00[b], 3.81[c], 3.79[d]	6.40[e], 6.64[f], 6.68[g], 7.00[h]
$H_5L^{5+} + H^+ \rightleftharpoons H_6L^{6+}$	3.40[a], 3.80[b], 3.26[c], 3.2[d]	5.67[e], 6.01[f], 6.05[g], 5.90[h]
$L + 6H^+ \rightleftharpoons H_6L^{6+}$	40.65[a], 43.15[b], 41.58[c], 41.39[d]	46.26[e], 47.71[f], 47.66[g], 47.90[h]

[a] I = 0.1 M NaTsO, Ref. [37].
[b] I = 0.1 M NMe_4Cl, Ref. [37].
[c] I = 0.1 M KNO_3, Ref. [38].
[d] I = 0.1 M KCl, average values from Refs. [39–44].
[e] I = 0.1 M in $NaClO_4$, Ref. [39].
[f] I = 0.1 M in $NaClO_4$, Ref. [39].
[g] I = 0.1 M in $NaMe_3PhSO_3$, Ref. [45].
[h] I = 0.1 M NaTsO, Ref. [46].

Table 4
Stepwise protonation (K_i^H) constants of **4m** and **4c** in aqueous solution; T = 298.15 K.

Equilibrium	$\log K_i^H$	
	4m[a]	**4c**
$L + H^+ \rightleftharpoons HL^+$	9.44	9.15[b], 9.2[c]
$HL^+ + H^+ \rightleftharpoons H_2L^{2+}$	8.68	8.88[b], 8.7[c]
$H_2L^{2+} + H^+ \rightleftharpoons H_3L^{3+}$	7.63	7.87[b], 8.0[c]
$H_3L^{3+} + H^+ \rightleftharpoons H_4L^{4+}$	6.46	6.79[b], 6.6[c]
$H_4L^{4+} + H^+ \rightleftharpoons H_5L^{5+}$	3.84	5.77[b], 5.93[c]
$H_5L^{5+} + H^+ \rightleftharpoons H_6L^{6+}$	3.18	5.00[b], 5.76[c]
$L + 6H^+ \rightleftharpoons H_6L^{6+}$	39.23	43.46[b], 44.2[c]

[a] I = 0.1 M KCl, Ref. [47].
[b] I = 0.1 M NaTsO, Ref. [47].
[c] I = 0.1 M Et_4NClO_4, Ref. [48].

Table 6
Stepwise protonation (K_i^H) constants of **6m** and **6c** in aqueous solution; T = 298.15 K.

Equilibrium	$\log K_i^H$	
	6m	**6c**
$L + H^+ \rightleftharpoons HL^+$	9.54[a], 9.54[b], 9.52[c]	9.6[d], 9.7[e,f]
$HL^+ + H^+ \rightleftharpoons H_2L^{2+}$	8.9[a], 8.76[b], 8.57[c]	9.00[d], 9.2[e,f]
$H_2L^{2+} + H^+ \rightleftharpoons H_3L^{3+}$	8.26[a], 8.16[b], 7.96[c]	8.62[d], 8.3[e,f]
$H_3L^{3+} + H^+ \rightleftharpoons H_4L^{4+}$	7.5[a], 7.26[b], 7.06[c]	7.4[d], 7.7[e,f]
$H_4L^{4+} + H^+ \rightleftharpoons H_5L^{5+}$	3.18[a], 3.3[b], 3.2[c]	6.7[d], 5.8[e]
$H_5L^{5+} + H^+ \rightleftharpoons H_6L^{6+}$	3.04[a], 2.5[b], –[c]	6.52[d], 5.68[e]
$L + 6H^+ \rightleftharpoons H_6L^{6+}$	40.42[a], 39.52[b], 36.31[c]	47.84[d], 46.38[e]

[a] I = 0.1 M KCl, Ref. [54].
[b] I = 0.1 M KCl, Ref. [55].
[c] I = 0.1 M KNO_3, Ref. [55].
[d] I = 0.1 M Et_3NClO_4, Ref. [49].
[e] I = 0.1 M NaTsO, Ref. [56].
[f] In this reference the authors do not provide values for this equilibrium. The values presented here where taken directly from the species distribution diagram provided in the supporting information of the reference.

protonated at a higher pH. The grouping effect discussed for the macrocycles is also attenuated for cryptands and what is observed is a steady drop in the magnitude of the protonation constants.

The remaining macrocycle/cryptand pairs [37–57] are of a different type where the two triamine units (in macrocycles) and the two tren units (in cryptands) are separated by a spacer (aliphatic or aromatic) which renders the two units more or less independent according to the size of the spacer, see Tables 3–7. In the case of the macrocycles the protonation occurs in the two triamine units in an alternated way giving rise to similar values of the protonation constants for the same protonation step in each subunit, differing only by the statistic factor. Therefore, the first four constants are higher and separated from the last two by several log units as the fifth and sixth protonation will occur in the central amine of each subunit, taking into accounts that in all the pairs the amine groups are separated by ethylene groups in each unit. The corresponding cryptands behave differently, with protonation constants usually dropping steadily throughout the protonation process and with

Table 5
Stepwise protonation (K_i^H) constants of **5m** and **5c** in aqueous solution; T = 298.15 K.

Equilibrium	$\log K_i^H$	
	5m	**5c**
$L + H^+ \rightleftharpoons HL^+$	9.49[a], 9.72[b]	10.5[c], 9.83[d], 9.59[e], 10.0[f], 10.27[g], 9.92[h]
$HL^+ + H^+ \rightleftharpoons H_2L^{2+}$	8.77[a], 8.96[b]	9.34[c], 9.25[d], 9.38[e], 9.1[f], 9.43[g], 9.26[h]
$H_2L^{2+} + H^+ \rightleftharpoons H_3L^{3+}$	8.04[a], 8.23[b]	8.59[c], 8.58[d], 8.80[e], 8.2[f], 8.57[g], 8.75[h]
$H_3L^{3+} + H^+ \rightleftharpoons H_4L^{4+}$	7.18[a], 7.51[b]	7.1[c], 7.13[d], 7.48[e], 7.29[f], 7.69[g], 7.67[h]
$H_4L^{4+} + H^+ \rightleftharpoons H_5L^{5+}$	3.51[a], 4.50[b]	6.2[c], 6.39[d], 6.77[e], 6.72[f], 6.7[g], 7.16[h]
$H_5L^{5+} + H^+ \rightleftharpoons H_6L^{6+}$	3.09[a], 3.50[b]	5.22[c], 5.58[d], 6.29[e], 6.54[f], 6.4[g], 6.59[h]
$H_6L^{6+} + H^+ \rightleftharpoons H_7L^{7+}$	–	2.85[e]
$L + 6H^+ \rightleftharpoons H_6L^{6+}$	40.08[a], 42.42[b]	46.95[c], 46.76[d], 48.31[e], 47.85[f], 49.06[g], 49.35[h]

[a] I = 0.1 M in $NaClO_4$, Ref. [50].
[b] I = 0.1 M in NaTsO, Ref. [51].
[c] I = 0.1 M in NaTsO, Ref. [52].
[d] I = 0.1 M NaTsO, Ref. [48].
[e] I = 0.1 M in NaTsO, Ref. [51].
[f] I = 0.1 M in $NaClO_4$, Ref. [52].
[g] I = 0.1 M in $NaNO_3$, Ref. [52].
[h] I = 0.1 M in KNO_3, Ref. [53].

Table 7
Stepwise protonation (K_i^H) constants of **7m** and **7c** in aqueous solution; T = 298.15 K.

Equilibrium	$\log K_i^H$	
	7m	**7c**
$L + H^+ \rightleftharpoons HL^+$	9.25[a]	9.4[b], 9.48[c]
$HL^+ + H^+ \rightleftharpoons H_2L^{2+}$	8.49[a]	8.8[b], 8.80[c]
$H_2L^{2+} + H^+ \rightleftharpoons H_3L^{3+}$	7.55[a]	7.8[b], 7.76[c]
$H_3L^{3+} + H^+ \rightleftharpoons H_4L^{4+}$	6.98[a]	7.1[b], 7.10[c]
$H_4L^{4+} + H^+ \rightleftharpoons H_5L^{5+}$	4.11[a]	6.4[b], 6.46[c]
$H_5L^{5+} + H^+ \rightleftharpoons H_6L^{6+}$	3.26[a]	5.4[b], 5.76[c]
$L + 6\,H^+ \rightleftharpoons H_6L^{6+}$	39.64[a]	44.9[b], 45.36[c]

[a] I = 0.1 M KCl, Ref. [57].
[b] I = 0.1 M Et_3NClO_4, Ref. [49].
[c] I = 0.1 M NaTsO, Ref. [48].

overall basicities always higher than their macrocyclic counterparts by several log units. The general observation is that in cryptands the positive charges can be better distributed around the cavity and the repulsion between ammonium positive charges attenuated.

3. Binding of anions by macrocyclic and cryptand receptors

3.1. Macrocycle *1m* and cryptand *1c*

Studies with Cl^-, Br^-, I^-, NO_3^-, ClO_4^- [30], IO_3^-, CF_3COO^-, $C_6H_5SO_3^-$ [58] and SO_4^{2-} [59] ions by potentiometric and conductometric measurements were reported by Zompa and coworkers for $H_n\mathbf{1m}^{n+}$ (n = 3 and 4) in aqueous solution. Association constants follow the trend $Cl^- > Br^- > I^-$ see Table 8 (the interaction with I^- is very weak), which are the expected ones if electrostatic interactions predominate. All the values are small except for SO_4^{2-}, for which a value of 4.12 was found. For all the anions, 1:1 receptor:anion species were found but for SO_4^{2-} and IO_3^- 1:2 stoichiometry also exists.

Thermodynamic functions were also determined, using the van't Hoff equation, from data of the binding constants at various temperatures [30,58,59]. These are one of the rare values for equilibria of anion associations. The data showed in general favorable entropic contributions and mostly unfavorable or slightly favorable enthalpic variations, see Tables 8 and 9. These data were interpreted as solvent ordering by the $H_n\mathbf{1m}^{n+}$ species and water loss from the receptor and anion solvation spheres. The authors emphasize that it is generally assumed that electrostatic and hydrogen-bonding interactions provide the binding forces in anion associations of protonated macrocyclic polyamines while the size and shape of the macrocyclic cavity account for binding selectivity, but they suggest that solvent release is an important driving force in these reactions [30]. Although the binding constant is larger for NO_3^- than Cl^-, in the solid state Cl^- forms stronger bonds to $H_4\mathbf{1m}^{4+}$. X-ray crystallographic analysis showed that one water molecule mediates between $H_4\mathbf{1m}^{4+}$ and NO_3^-, while Cl^- interacts directly with the ammonium sites [30]. These crystallographic features are apparently in agreement with the thermodynamic data since a higher solvation of the Cl^- anion leads the association reaction to be more endothermic and more entropically favored than in the case of the NO_3^- ion [30].

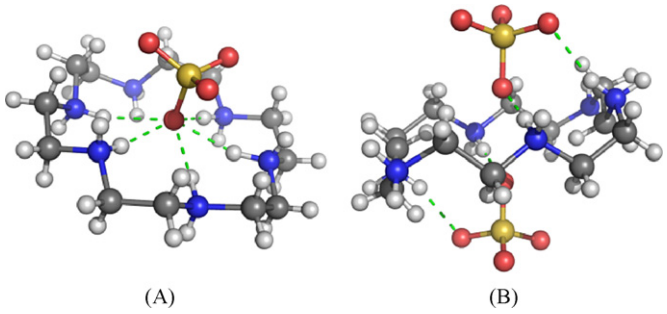

Fig. 1. Crystal structures of the association of $H_6\mathbf{1m}^{6+}$ and sulfate, obtained by addition of conc. H_2SO_4 to **1m** (A), and by the same procedure but adjusting the pH at 2 with NaOH (B) [66].

Kimura and coworkers used also $H_n\mathbf{1m}^{n+}$ as receptor for binding studies of many anions, in all cases they worked at neutral aqueous solution and then the receptor was in the $H_3\mathbf{1m}^{3+}$ form. Anions such as mono-, di- and tri-carboxylates [60], carbonate [61], HPO_4^{2-} and the nucleotides AMP^{2-}, ADP^{3-} and ATP^{4-} [62], catechol and its derivatives [63], were studied. These results were not considered in this review as the authors restricted the studies to a very small pH region.

An extensive binding study of phosphate and pyrophosphate, and later of sulfate, with $H_n\mathbf{1m}^{n+}$ was carried out in aqueous solution by potentiometry and microcalorimetry, see values in Table 9 [29,64]. The sulfate binding affinity with $H_4\mathbf{1m}^{4+}$ is the only common case in the studies of the Florence group and Zompa and coworkers, and in spite that the main conclusions that can be derived from the values of both groups are the same, the individual values are very discrepant. In an earlier report García-España and coworkers studied the binding of $H_n\mathbf{1m}^{n+}$ with $P_2O_7^{4-}$, ATP^{4-} and $[Fe(CN)_6]^{4-}$, in which some stepwise constants are not in agreement with the K_{eff} values [65]. For $P_2O_7^{4-}$, the values were corrected later [29] but to the best of our knowledge no other report with ATP^{4-} and $H_n\mathbf{1m}^{n+}$ was published.

The binding constants for SO_4^{2-} increase with increasing positive charge (number of protons) on the receptor indicating that electrostatic attraction is the principal force that determines the stability of these anionic associations, although hydrogen bonding between the anions and the polyammonium receptor is expected to give a favorable contribution, see below. Hence, the amount of bound anion increases with decreasing pH [29].

Crystal structures of the association of sulfate with $H_6\mathbf{1m}^{6+}$ were reported; see Fig. 1 [66]. They reveal that the $H_6\mathbf{1m}^{6+}$ form of the receptor can bind sulfate through several hydrogen bonds, although this species only can be formed at extremely acidic pH.

For phosphate and pyrophosphate the binding interactions of the association are not strictly determined by electrostatic contributions. Indeed, for a given protonation state of the receptor, less charged anions can form more stable associated species. Of especial

Table 8
Association constants ($\log K_{H_hL_lA_a}$) of $H_4\mathbf{1m}^{4+}$ with several anions in aqueous solution; T = 298.15 K, I = 0.21 M in NaCl + $NaNO_3$ [30,58].

Equilibrium	$\log K_{L_lH_hA_a}$	ΔH, kcal mol^{-1}	$T\Delta S$, kcal mol^{-1}
$H_4\mathbf{1m}^{4+} + Cl^- \rightleftharpoons [H_4\mathbf{1m}Cl]^{3+}$	1.86	4.9	7.2
$H_4\mathbf{1m}^{4+} + Br^- \rightleftharpoons [H_4\mathbf{1m}Br]^{3+}$	1.46	–	–
$H_4\mathbf{1m}^{4+} + NO_3^- \rightleftharpoons [H_4\mathbf{1m}NO_3]^{3+}$	2.32	−0.4	3.6
$H_4\mathbf{1m}^{4+} + ClO_4^- \rightleftharpoons [H_4\mathbf{1m}ClO_4]^{3+}$	1.04	−2.5	−1.1
$H_4\mathbf{1m}^{4+} + C_6H_5SO_3^- \rightleftharpoons [H_4\mathbf{1m}C_6H_5SO_3]^{3+}$	0.5	6.6	7.3
$H_4\mathbf{1m}^{4+} + CF_3CO_2^- \rightleftharpoons [H_4\mathbf{1m}CF_3CO_2]^{3+}$	0.91	6.5	7.7
$H_4\mathbf{1m}^{4+} + IO_3^- \rightleftharpoons [H_4\mathbf{1m}IO_3]^{3+}$	2.78	1.3	5.1
$H_4\mathbf{1m}^{4+} + 2\,IO_3^- \rightleftharpoons [H_4\mathbf{1m}(IO_3)_2]^{2+}$	3.86	−1.0	4.3

Table 9
Stepwise association constants ($\log K_{H_hL_lA_a}$) of $H_n\mathbf{1m}^{n+}$ with sulfate, phosphate and pyrophosphate anions in aqueous solution; $T = 298.15$ K.

Equilibrium	$\log K_{L_lH_hA_a}$	ΔH, kcal mol^{-1}	$T\Delta S$, kcal mol^{-1}
$H_5\mathbf{1m}^{5+} + SO_4^{2-} \rightleftharpoons [H_5\mathbf{1m}SO_4]^{3+}$	4.44[a]	1.4[a]	7.4[a]
$H_4\mathbf{1m}^{4+} + SO_4^{2-} \rightleftharpoons [H_4\mathbf{1m}SO_4]^{2+}$	3.84[a], 4.12[b]	−1.6[a], 5.6[b]	3.6[a], 11.3[b]
$H_4\mathbf{1m}^{4+} + 2\,SO_4^{2-} \rightleftharpoons [H_4\mathbf{1m}(SO_4)_2]$	5.90[b]	7.7[b]	15.9[b]
$H_3\mathbf{1m}^{3+} + SO_4^{2-} \rightleftharpoons [H_3\mathbf{1m}SO_4]^{+}$	1.64[b]	2.8[b]	5.0[b]
$H_2\mathbf{1m}^{2+} + SO_4^{2-} \rightleftharpoons [H_2\mathbf{1m}SO_4]$	2.79[a]	−0.7[a]	3.1[a]
$H_5\mathbf{1m}^{5+} + H_2PO_4^{-} \rightleftharpoons [H_7\mathbf{1m}PO_4]^{4+}$	5.53[c]	−5.4[c]	2.1[c]
$H_4\mathbf{1m}^{4+} + H_2PO_4^{-} \rightleftharpoons [H_6\mathbf{1m}PO_4]^{3+}$	5.02[c]	0.3[c]	7.1[c]
$H_3\mathbf{1m}^{3+} + H_2PO_4^{-} \rightleftharpoons [H_5\mathbf{1m}PO_4]^{2+}$	3.71[c]	−2.9[c]	2.1[c]
$H_3\mathbf{1m}^{3+} + HPO_4^{2-} \rightleftharpoons [H_4\mathbf{1m}PO_4]^{+}$	2.69[c]	1.1[c]	4.8[c]
$H_5\mathbf{1m}^{5+} + H_2P_2O_7^{2-} \rightleftharpoons [H_7\mathbf{1m}P_2O_7]^{3+}$	4.11[c]	1.4[c]	7.0[c]
$H_4\mathbf{1m}^{4+} + H_2P_2O_7^{2-} \rightleftharpoons [H_6\mathbf{1m}P_2O_7]^{2+}$	4.37[c]	−1.3[c]	4.7[c]
$H_3\mathbf{1m}^{3+} + H_2P_2O_7^{2-} \rightleftharpoons [H_5\mathbf{1m}P_2O_7]^{+}$	4.04[c]	−9.7[c]	−4.2[c]
$H_4\mathbf{1m}^{4+} + HP_2O_7^{3-} \rightleftharpoons [H_5\mathbf{1m}P_2O_7]^{+}$	5.69[c,d]	2.3[c]	10.1[c]
$H_3\mathbf{1m}^{3+} + HP_2O_7^{3-} \rightleftharpoons [H_4\mathbf{1m}P_2O_7]$	3.27[c]	−6.6[c]	−2.1[c]
$H_3\mathbf{1m}^{3+} + P_2O_7^{4-} \rightleftharpoons [H_3\mathbf{1m}P_2O_7]^{-}$	2.94[c]	1.2[c]	5.2[c]

[a] $I = 0.15$ M in $NaClO_4$, Ref. [64].
[b] $I = 0.21$ M in NaCl + $NaNO_3$, Ref. [59].
[c] $I = 0.15$ M in $NaClO_4$, Ref. [29].
[d] This constant is not supported by K_{eff} values.

importance is the ability of phosphate and pyrophosphate anions to behave as acceptors and donors of hydrogen bonds [29].

In agreement to a simple electrostatic model, the formation of ion pairs between rigid cations and anions (hard sphere with embedded point charges) in an ideal, structureless homogeneous, solvent is expected to be accompanied by slightly unfavorable ΔH° contributions and largely favorable entropic terms. This is principally derived from desolvation of the interacting species determined by the charge neutralization occurring in the pairing process. In agreement with this model, most of the association reactions involving sulfate, phosphate and pyrophosphate anions are almost athermic, or endothermic, and show favorable entropic contributions ($T\Delta S^\circ > 0$), although there is also some reactions with phosphate and pyrophosphate promoted by favorable enthalpy changes ($\Delta H^\circ < 0$) and entropy loss [29,64].

Polyammonium receptors can bind phosphate or $P_2O_7^{4-}$ anions forming associations *via* many hydrogen bonds in which both the anions and the receptor can act as acceptors or donors. Following García-España and coworkers four possible modes of hydrogen bonding (type 1) involving amine or ammonium groups as donors, and just one (type 2) involving the amine groups as acceptors in the formation of the anion associations can be considered, see below, being 1.1, 1.2, and 2 the expected principal hydrogen binding modes, depending on the structure and the protonation degree of the interacting species [29]:

$$\text{–N–H}^{+}\cdots{}^{-}\text{O–} \quad \Delta H^\circ > 0, \ T\Delta S^\circ > 0 \tag{1.1}$$

$$\text{–N}^{+}\text{–H}\cdots\text{OH–} \quad \Delta H^\circ > 0, \ T\Delta S^\circ \approx 0 \tag{1.2}$$

$$\text{–N–H}\cdots{}^{-}\text{O–} \quad \Delta H^\circ > 0, \ T\Delta S^\circ \approx 0 \tag{1.3}$$

$$\text{–N–H}\cdots\text{OH–} \quad \Delta H^\circ > 0, \ T\Delta S^\circ < 0 \tag{1.4}$$

$$\text{–N}:\cdots\text{H–O–} \quad \Delta H^\circ < 0, \ T\Delta S^\circ < 0 \tag{2}$$

Spiccia and cowokers reported a series of crystal structures of $H_4\mathbf{1m}^{4+}$ and $H_nPO_4^{n-3}$ (Fig. 2) [67]. All the structures represent species that were not expected to be obtained at the pH of synthesis of the crystals and (C in Fig. 2) is not at all found in the solution studies. Apparently arrangements of the receptor with symmetric ammonium ions crystallize more readily from solution, as there are no reported structures having $H_5\mathbf{1m}^{5+}$ or $H_3\mathbf{1m}^{3+}$ as receptors. Hydrogen bonds of types 1.2 and 2 were not found in this set of crystal structures.

It is necessary to have in mind when comparing solution and crystal structures studies that "the decisive reason not to take X-ray crystal structures too seriously stems from the omission of entropy" [4]. Considering the crystal structure as the unique in solution is a broad simplification of a complex process where only a collection of individual arrangements represents the structural ensemble, even if the configuration of the assembled molecule observed in the crystal is the most stable one in solution [4].

As the protonation of SO_4^{2-} is an endothermic reaction ($\approx$5 kcal mol^{-1}) it is expected more favorable enthalpic contribution on hydrogen-bonding formation in modes (1.1) and (1.3) in phosphate than in sulfate associations. Therefore the binding of sulfate by $H_n\mathbf{1m}^{n+}$ is mostly determined by largely favorable entropic terms produced by the desolvation of the interacting species, which

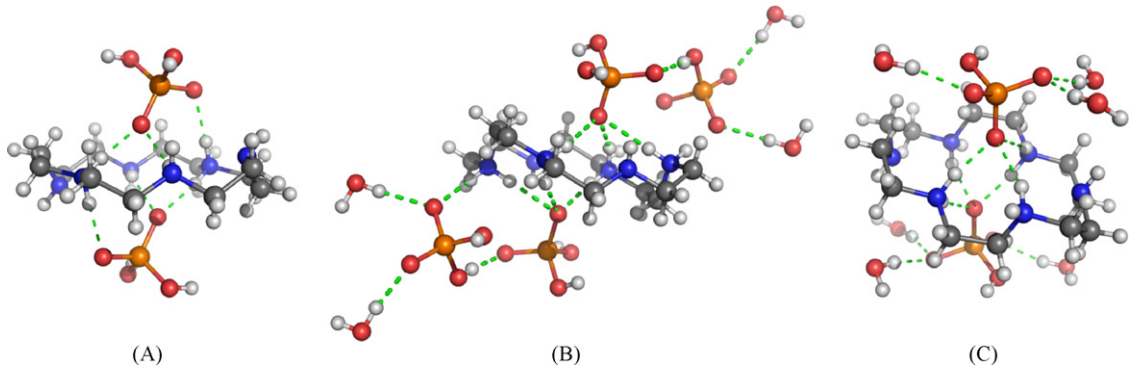

Fig. 2. Crystal structures of the associations between $H_4\mathbf{1m}^{4+}$ and $H_nPO_4^{n-3}$ obtained at pH 6 (A and B) and at pH 8 (C) [67].

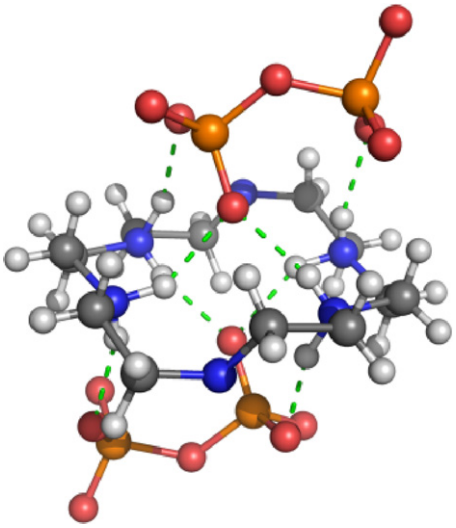

Fig. 3. Crystal structure of the association of $H_4\mathbf{1m}^{4+}$ with $H_2P_2O_7^{2-}$ [29].

occurs as a consequence of the charge neutralization that accompanies the pairing process [64].

The crystal structure of $H_4\mathbf{1m}^{4+}$ with $H_2P_2O_7^{2-}$ is represented in Fig. 3, where the protonated macrocycle adopts an almost planar arrangement with the nitrogen atoms in *endo* conformation. The $H_2P_2O_7^{2-}$ are facially bound to the receptors in a sandwich-like fashion, forming long N–H···O–P–O–P–O···H–N hydrogen-bonded bridges. The only other interactions in the packing involve the water solvent molecules and the $H_2P_2O_7^{2-}$ anions belonging to different units.

On the other hand, the binding affinity of F^- and Cl^- with the $H_6\mathbf{1c}^{6+}$ cryptand was studied and the binding constants were determined by potentiometry, see Table 10, and by NMR experiments (^{1}H and ^{13}C NMR). The authors studied the structures of the cryptand and its association with fluoride and the dynamics of fluoride proton exchange [31]. The $H_6\mathbf{1c}^{6+}$ is the most protonated form of the receptor observed. The authors propose that above pH 4 (four protonation constants) the secondary amines are oriented internal to the cryptand cavity and participate in an intramolecular hydrogen bond network, and below pH 4, this hydrogen bond network is at least partially disrupted. The ^{1}H NMR data provide strong evidence for a substantial conformational change upon protonation of $H_4\mathbf{1c}^{4+}$. This conformational change breaks the internal hydrogen bonds and rotates the amines external to the cavity. The conformational change helps to reduce electrostatic repulsions and simultaneously enables increased internal van der Waals interactions of the hydrocarbon chains [31]. The X-ray structure of **1c** at high pH exhibits crystallographic D_3 symmetry and shows the protonated secondary amines involved in a hydrogen-bonding network of surrounding water molecules [68]. The two tertiary amines along the three-fold axis are 6.37 Å apart and have their lone pairs directed towards the centre of the cavity, thus shielded from significant interaction with solvent. The N–H protons are directed towards the centre of the cavity, and with adjacent N···N distances of 2.93–3.04 Å, which is well within the range of typical N–H···N hydrogen bonds.

The cryptand exhibits an extraordinary selectivity for F^- over Cl^- (about 7 orders of magnitude) see Table 10. The crystal structure of the fluoride cryptate [69] and the magnitude of the fluoride binding constant with $H_6\mathbf{1c}^{6+}$ strongly suggest that this anion binds inside the cryptand cavity in aqueous solution. The ^{1}H NMR spectrum of the cryptand exhibits large shifts upon addition of F^- and small ones upon addition of Cl^- (relative to nitrate) suggesting that chloride does not bind inside the cavity.

The crystal structure shows the F^- anion located inside the cavity of the receptor forming N–H···F hydrogen bonds with the six ammonium nitrogen protons in a quasi-trigonal prismatic geometry, see Fig. 4A. The bridgehead nitrogen atoms are not protonated and are not involved in the binding. The median N–F distance of 2.81 Å which is typical of N–H···F hydrogen bonds, and the distance from the cavity centre to all secondary amines in the crystal structure of the free ligand is 2.82 Å. Thus, the selectivity is primarily associated with the ideal match of the cryptand cavity with the size of the F^- ion [31,32].

The overall magnitude of F^- binding and the F^-/Cl^- selectivity of this cryptand in water are unprecedented. The pH-controlled reversibility of fluoride binding in the cryptand system yields an important advantage when applications in separations chemistry are considered [31,32].

Later, Bowman-James and coworkers [70,71] showed by single crystal X-ray diffraction that $H_6\mathbf{1c}^{6+}$ can also encapsulate the Cl^- anion. The crystal showed a single Cl^- ion inside the cavity (Fig. 4B), while the remaining five and water molecules are outside. The cavity is only slightly smaller in the $[H_6\mathbf{1c}Cl]^{5+}$ supermolecule (the apical N···N distance is of 6.60 Å, compared to 6.65 Å in the fluoride one). The chloride is held tightly, not symmetrically, by a hydrogen bond network with the six amine nitrogen atoms, with distances ranging from 2.99 to 3.18 Å. The distances of the chloride to the apical nitrogen atoms are 3.27 and 3.32 Å. ^{1}H NMR titration with F^-, Cl^-, Br^- and I^- at 4.0 pD value showed no association with Cl^- [70], however, the log *K*s for Cl^- binding at pD 2.0 is 2.86, which is about one order of magnitude higher than the value obtained by potentiometric methods (see Table 10). The NMR spectra of other halides and nitrate at ca. pD 2.0 indicated little changes from that observed for the receptor, $H_6\mathbf{1c}(TsO)_6$, suggesting that only fluoride and chloride are able to be encapsulated by the receptor. In fact, the cryptand **1c** titrated with HI crystallizes as $[H_4\mathbf{1c}(H_2O)][I]_4{\cdot}4H_2O$, where one water molecule sits inside the cryptand cavity, Fig. 4D. The encapsulated water molecule exhibits tetrahedral coordination, forming two O···H–N (the oxygen of the water and hydrogen atoms of two nitrogen atoms of different chains of **1c**) and two O–H···N (water protons and the two amine lone pairs) hydrogen bonds. These hydrogen bonds are the shortest to the encapsulated water. More recently a study by Ghosh and coworkers [72] showed that the hexaprotonated form of **1c** crystallizes as $[H_6\mathbf{1c}][Br]_6{\cdot}H_2O$ without any Br^- anion encapsulated (Fig. 4C). Furthermore, this study complements the previous findings showing the selective encapsulation of fluoride over chloride and of chloride over bromide in the solid state.

In conclusion, the $H_n\mathbf{1c}^{n+}$ cryptand is extremely selective for the small F^- anion at pH values >2, although for lower pH values Cl^- competes with F^- to be encapsulated into the cavity [69,70]. The binding affinity of F^- is very high, the log K_{eff} increases with the decrease of pH being about 9.3 at pH 2.5. On the other hand, the

Table 10
Stepwise association constants ($\log K_{H_hL_jA_a}$) of $H_n\mathbf{1c}^{n+}$ with fluoride and chloride in aqueous solution; T = 298.15 K.

Equilibrium	$\log K_{L_jH_hA_a}$	
	A = F^-	A = Cl^-
$H_3\mathbf{1c}^{3+} + A^- \rightleftharpoons [H_3\mathbf{1c}A]^{2+}$	3.6[a], 3.30[b]	–
$H_4\mathbf{1c}^{4+} + A^- \rightleftharpoons [H_4\mathbf{1c}A]^{3+}$	5.1[a], 5.20[b]	–
$H_5\mathbf{1c}^{5+} + A^- \rightleftharpoons [H_5\mathbf{1c}A]^{4+}$	≥8.8[a,c], 8.40[b]	≥1.2[a,c], 2.8[d]
$H_6\mathbf{1c}^{6+} + A^- \rightleftharpoons [H_6\mathbf{1c}A]^{5+}$	11.2[a], 10.55[b]	<2[b]

[a] I = 0.1 M in KNO_3, Ref. [31].
[b] I = 0.1 M in Me_4NTsO, Ref. [32].
[c] These values were estimated by assuming that the two-proton reaction, $LH_4^{4+} + 2\,H^+ \rightleftharpoons LH_6^{6+}$, can be divided into two single-proton equilibria, in which the first constant is ≥4.39/2, and the sum of both constants is 4.39.
[d] ^{1}H NMR experiments at pD = 2.0 [70].

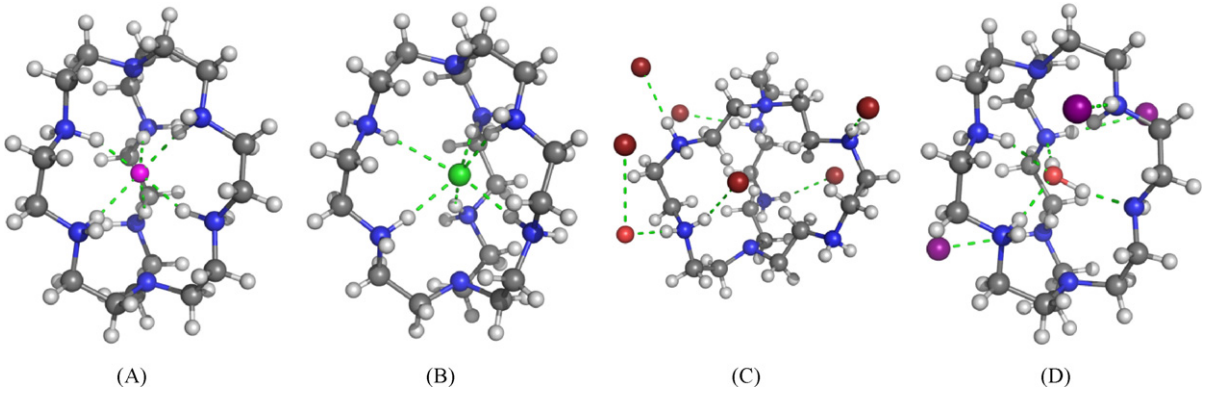

Fig. 4. Crystal structures of the supermolecules formed by F^- (A) [32] and Cl^- (B) [70] anions with $H_6\mathbf{1c}^{6+}$ receptor, in (C) of $H_6\mathbf{1c}^{6+}$ in presence of Br^- [72] with the Br^- anions outside the cavity, and in (D) the structure of the included H_2O into the cavity of $H_4\mathbf{1c}^{4+}$ receptor with several iodide anions outside the cavity [71], see text.

macrocycle, $H_n\mathbf{1m}^{n+}$, can bind a large variety of anions but without any particular selectivity.

3.2. Macrocycle *2m* and cryptand *2c*

The $H_n\mathbf{2m}^{n+}$ receptor forms with Cl^- and SO_4^{2-} weaker associations than the analogous $H_n\mathbf{1m}^{n+}$. The propylenic chains connecting the amino groups in **2m** allow its complete protonation at higher pH values but the receptor has a reduced charge density and then weaker binding affinity for anions than $H_n\mathbf{1m}^{n+}$ with ethylenic chains, see Tables 2 and 12.

The comparison of the $H_n\mathbf{2m}^{n+}$ macrocycle/$H_n\mathbf{2c}^{n+}$cryptand behaviors shows that whereas the binding of halides by $H_6\mathbf{2m}^{6+}$ is very weak, the $H_n\mathbf{2c}^{n+}$ is capable to bind Cl^-, Br^- and I^- following the trend $I^- > Br^- > Cl^-$, indicating that the halide binding is not governed only by electrostatic interactions but the match of sizes of the cavity and the substrate should also play an important role, see Table 11. In fact, the large and spherical cavity with an almost symmetrical distribution of charged sites of $H_8\mathbf{2c}^{8+}$ may accommodate well the spherical and smaller charge density I^- anion. Unfortunately structural information is not available [33,35]. However $H_8\mathbf{2c}^{8+}$ is unable to discriminate I^- from a mixture of the three halides as shown in Fig. 5a, even though it exhibits a clear preference for the larger anion. On the other hand, if SO_4^{2-} is added to the mixture of halides this cryptand selectively uptakes the sulfate from the aqueous solution, as shown in Fig. 5b.

Interesting is also to verify that the macrocycle $H_n\mathbf{2m}^{n+}$ is just as effective in separating SO_4^{2-} from Cl^-, Br^- and I^-, or even more, as the cryptand. Indeed the $H_n\mathbf{2m}^{n+}$ binds the halides so weakly that the binding constants cannot be accurately measured by potentiometry while sulfate is bound as strongly as by the $H_6\mathbf{2c}^{6+}$ cryptand ($\log K_{[H_6\mathbf{2m}(SO_4)]} = 4.05$ and $\log K_{[H_6\mathbf{2m}(SO_4)]} = 4.20$).

The association constants determined in water by pH-meter measurements showed that $H_n\mathbf{2m}^{n+}$ also forms stable 1:1 associations with carboxylates, nucleotide (AMP^{2-}, ADP^{3-} and ATP^{4-}), $Fe(CN)_6^{4-}$ and $Co(CN)_6^{3-}$ anions, see Table 12 and the $\log K_{eff}$ *versus* pH in Fig. 6 [33,35,73–75]. The binding affinity of the associations increases with the charge of the anion and with the charge of the receptor. These trends agree with a predominant electrostatic contribution to the interaction between these anions and the polyammonium receptors. Indeed, among the studied carboxylates, citrate presents the larger affinity for $H_6\mathbf{2m}^{6+}$. In the dicarboxylate series, it is clear from Fig. 6 that oxa^{2-} is the strongest bound anion followed by mal^{2-}. On other hand, suc^{2-}, glu^{2-} and ad^{2-} anions are too long or flexible for the $H_n\mathbf{2m}^{n+}$ cavity, and a drop in the value of the binding constants is observed. For abbreviations of anions see below before references.

A closer observation at the dicarboxylate anions with two carbon atoms between the carboxylate groups, Fig. 6 dashed lines, reveals that suc^{2-}, tar^{2-} and fum^{2-} have about the same effective constant at pH 6 whereas $male^{2-}$ has a value about 1 log unit higher and of about the same magnitude of that of mal^{2-}, in agreement with the fact that $male^{2-}$ has the carboxylate groups at a shorter distance as they are in *cis* conformation.

Despite the preferences of $H_n\mathbf{2m}^{n+}$ for dicarboxylates described above, it is clear from the distribution diagrams of Fig. 7 that this receptor is not as selective as the cryptand. The authors claimed that the superiority of $H_n\mathbf{2c}^{n+}$ is based on a better fit of oxa^{2-} into the cavity and on an incomplete encapsulation of mal^{2-} anion.

Table 11
Stepwise ($\log K_{H_hL_lH_hA_a}$) association constants of $H_n\mathbf{2c}^{n+}$ with the halides in aqueous solution, $T = 298.15$ K.

Equilibrium[a]	log $K_{L_lH_hA_a}$		
	A = Cl^-	A = Br^-	A = I^-
$H_8\mathbf{2c}^{8+} + A^- \rightleftharpoons [H_8\mathbf{2c}A]^{7+}$	2.40	2.95	3.40
$H_7\mathbf{2c}^{7+} + A^- \rightleftharpoons [H_7\mathbf{2c}A]^{6+}$	2.10	2.65	3.00
$H_6\mathbf{2c}^{6+} + A^- \rightleftharpoons [H_6\mathbf{2c}A]^{5+}$	1.70	2.20	2.40
$H_5\mathbf{2c}^{5+} + A^- \rightleftharpoons [H_5\mathbf{2c}A]^{4+}$	1.50	1.70	1.95

[a] $I = 0.1$ M in NaTsO [35].

Table 12
Stepwise ($\log K_{H_hL_lA_a}$) association constants for the indicated equilibrium in aqueous solution; $T = 298.15$ K.

Equilibrium	log $K_{H_hL_lA_a}$	
	L = **2m**	L = **2c**[a]
$H_8L^{8+} + SO_4^{2-} \rightleftharpoons [H_8LSO_4]^{6+}$	–	7.45
$H_7L^{7+} + SO_4^{2-} \rightleftharpoons [H_7LSO_4]^{5+}$	–	5.60
$H_6L^{6+} + SO_4^{2-} \rightleftharpoons [H_6LSO_4]^{4+}$	4.05[b]	4.20
$H_5L^{5+} + SO_4^{2-} \rightleftharpoons [H_5LSO_4]^{3+}$	3.05[b]	3.20
$H_4L^{4+} + SO_4^{2-} \rightleftharpoons [H_4LSO_4]^{2+}$	2.50[b]	2.75
$H_8L^{8+} + oxa^{2-} \rightleftharpoons [H_8Loxa]^{6+}$	–	6.55
$H_7L^{7+} + oxa^{2-} \rightleftharpoons [H_7Loxa]^{5+}$	–	5.20
$H_6L^{6+} + oxa^{2-} \rightleftharpoons [H_6Loxa]^{4+}$	3.80[b]	4.50
$H_5L^{5+} + oxa^{2-} \rightleftharpoons [H_5Loxa]^{3+}$	3.20[b]	3.25
$H_4L^{4+} + oxa^{2-} \rightleftharpoons [H_4Loxa]^{2+}$	2.60[b]	–
$H_8L^{8+} + mal^{2-} \rightleftharpoons [H_8Lmal]^{6+}$	–	4.00 (2.88*)
$H_7L^{7+} + mal^{2-} \rightleftharpoons [H_7Lmal]^{5+}$	–	3.10
$H_6L^{6+} + mal^{2-} \rightleftharpoons [H_6Lmal]^{4+}$	3.30[b]	2.85
$H_5L^{5+} + mal^{2-} \rightleftharpoons [H_5Lmal]^{3+}$	2.60[b]	2.20
$H_4L^{4+} + mal^{2-} \rightleftharpoons [H_4Lmal]^{2+}$	2.45[b]	–

[a] $I = 0.1$ M NaTsO, Ref. [35].
[b] $I = 0.1$ M Me_4NCl, Ref. [35].
* Value in agreement with the K_{eff} *versus* pH diagram, Fig. 6, indicating that for this value the correct equilibrium was not ascribed by the authors, instead it is $H_7L^{7+} + Hmal^- \rightleftharpoons [H_8Lmal]^{6+}$ because the K_{eff} value decrease for pH values lower than 5.

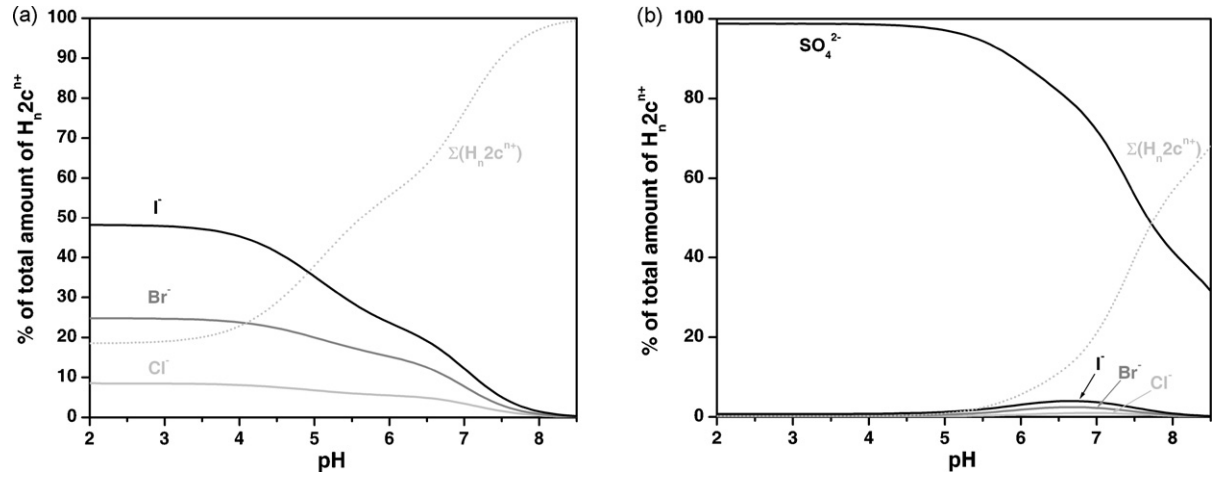

Fig. 5. Distribution diagrams of the overall amount of supramolecular species formed between $H_n\mathbf{2c}^{n+}$ and the mixture of halide anions, Cl^-, Br^- and I^- in the 1:1:1:1 ratio (a) and a mixture of the halides and sulfate (b). $C_{cryp} = C_A = 2 \times 10^{-3}$ M. Note: for simplicity the amount of associated species with each anion is identified in the diagrams only by the formula of the anions, Cl^-, Br^-, I^-, and SO_4^-, respectively in this case.

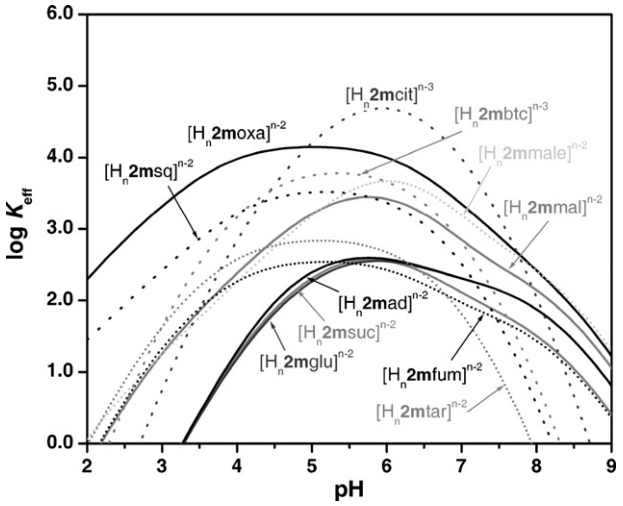

Fig. 6. Plots of the effective association constant K_{eff} (in log units) *versus* pH for the associations formed between $H_n\mathbf{2m}^{n+}$ and the indicated carboxylate anions, based on reported association constants [33,35,73–75]. $C_{\mathbf{2m}} = C_A = 2 \times 10^{-3}$ M.

Furthermore, the $H_n\mathbf{2m}^{n+}$ was found to bind strongly nucleotides, especially ATP^{4-} (the maximum $\log K_{eff}$ is 8.3 at pH 6.5), as it is able to be fully protonated at the pH region where ATP^{4-} is completely deprotonated [75], taking advantage of strong electrostatic interactions. At the same pH, the $\log K_{eff}$ is 6.0 for ADP^{3-} and 3.0 for AMP^{2-}. The interaction of the cryptand with the nucleotides was not studied.

Moreover, the data of Table 12 allow the evaluation of the binding preference of SO_4^{2-} or oxa^{2-} and mal^{2-} dianions for the pair of receptors $H_n\mathbf{2m}^{n+}/H_n\mathbf{2c}^{n+}$ along the pH values. The results are shown for SO_4^{2-} in Fig. 8a (oxa^{2-} has a similar behavior) and for mal^{2-} in Fig. 8b. The SO_4^{2-} and oxa^{2-} clearly prefer $H_n\mathbf{2c}^{n+}$, being selective for the cryptand at low pH values (up to about 4). Mal^{2-} presents a very different behavior for which $H_n\mathbf{2m}^{n+}$ is preferred, especially in the pH range 5–7. These results indicate that the size, the geometry and the rigidity of the anion are important features for the selective accommodation of the substrate into the cavity of the cryptand. The complete lack of structural data for associated molecules of this pair of receptors with anions prevents us to go further in the structural analysis.

3.3. *Macrocycle **3m** and cryptand **3c***

The $H_n\mathbf{3m}^{n+}$ macrocycle is one of the most used receptor in associations with anions, even though with monoanions only Br^-

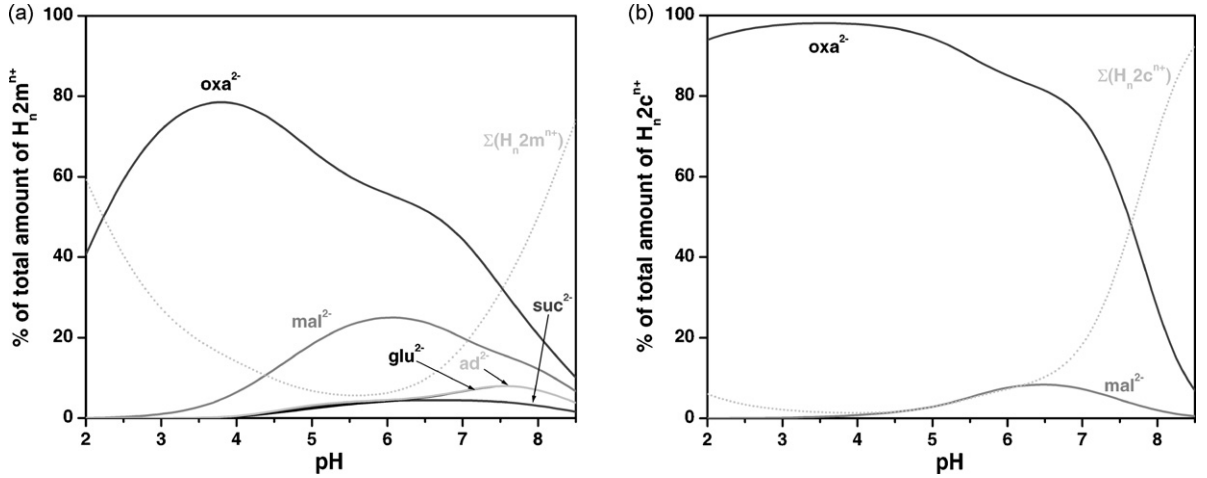

Fig. 7. Distribution diagrams of the overall amounts of supramolecular species formed between $H_n\mathbf{2m}^{n+}$ (a) and $H_n\mathbf{2c}^{n+}$ (b) with the indicated anions in equimolar ratio. $C_{\mathbf{2m}} = C_{\mathbf{2c}} = C_A = 2 \times 10^{-3}$ M. See note of Fig. 5.

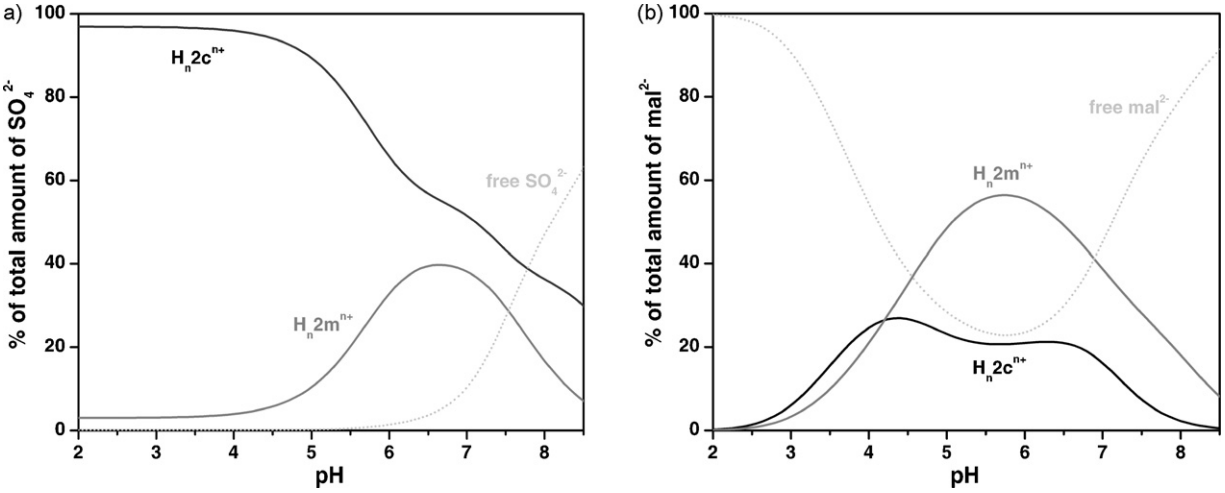

Fig. 8. Distribution diagram of the overall amounts of supramolecular species formed between SO_4^{2-} (a) and mal^{2-} (b) with protonated receptors, H_n**2m**$^{n+}$ and H_n**2c**$^{n+}$ in equimolar ratio. $C_{\mathbf{2c}} = C_{\mathbf{2m}} = C_A = 2 \times 10^{-3}$ M.

[76] has binding constants reported, see Table 13. The protonation constants determined in an "inert" medium as NaTsO [37] present lower values for $\log K_4^H$ than in media containing chloride or nitrate, indicating that these two anions interact with H_n**3m**$^{n+}$. In spite of knowing this fact almost all the values of association constants of the literature were obtained in 0.1 M KCl medium.

X-ray crystal structures of chloride and nitrate associations with H_n**3m**$^{n+}$ were reported. In the crystal structure H_6**3m**$^{6+}$6Cl^-·4H_2O [37], the receptor adopts a pocket-like conformation with the oxygen atoms of the ring above the mean plane of the nitrogen atoms, see Fig. 9A. Each proton of the six nitrogen atoms is involved in short contacts with Cl^- anions and/or water molecules. Most of the protons of the six ammonium groups are turned towards the centre of the "pocket". Among the three closest anions, one of them, interacting unsymmetrically with four ammonium groups, is located in the centre of the macrocycle and bound by four ammonium groups with N···Cl^- distances of less than 3.4 Å [37]. In the crystal with nitrate, the macrocycle is in the H_4**3m**$^{4+}$ form, leaving the two lone pairs on the central amines available. Bond distances clearly indicate hydrogen-bonding interactions between the nitrate and the cationic macrocycle. The nitrate is held in a 4-fold hydrogen-bonding network, see Fig. 9B [77].

An almost reversed situation occurs with the corresponding cryptand, **3c**, for which NaTsO salt was used for the determinations of association constants of all the halides, nitrate and azide anions, see Table 13. Among the monovalent anions, F^- and N_3^- display the highest binding constants with H_6**3c**$^{6+}$, the trend for the monoanions studied being $ClO_4^- < I^- < HCO_2^- < Br^- < NO_3^- < Cl^- < F^- < N_3^-$ [46]. The highest constants found for F^-, in comparison with the other halides, is due to its high charge density. Very interesting X-ray structures of H_6**3c**$^{6+}$ with F^-, Cl^-, Br^- and N_3^- (Fig. 10) revealed the topological discrimination of the receptor [46,78]. In [H_6**3c**F]5ClO_4·1/2H_2O, the small F^- cannot bind equivalently to the six protons and slides towards one side of the cavity, bound in a tetrahedral fashion to four protonated N atoms. The anion is situated well outside the bridgehead NN axis at average F···N distance of 2.72 Å. In the [H_6**3c**Cl]$^{5+}$ and [H_6**3c**Br]$^{5+}$ crystal structures one anion is included. The encapsulated Cl^- and Br^- ions establish hydrogen bonds to the six protonated secondary N atoms in octahedral fashion and are located exactly on the NN axis joining the two bridgehead N atoms and at equal distance from them: Cl···N = 3.72 Å and Br···N = 3.76 Å. Finally, in the crystal [H_6**3c**N_3]4PF_6Cl·3H_2O, the linear N_3^- occupies the cavity, the anion is located in the bridgehead NN axis, and the two terminal N atoms of N_3^- are at 3.34 and 3.21 Å from the N atoms of the receptor. The receptor is markedly expanded around the enclosed N_3^- and the geometrical requirements of the cavity are apparently fulfilled [46,78].

On the other hand, a large series of polycharged anions were studied with this pair of receptors in aqueous solution, those that can be compared are compiled in the Table 14

Table 13
Stepwise (log $K_{H_hL_lA_a}$) association constants for the indicated equilibrium in aqueous solution. T = 298.15 K.

Equilibrium[a]	$\log K_{H_hL_lA_a}$	
	L = **3m**	L = **3c**
$H_6L^{6+} + F^- \rightleftharpoons [H_6LF]^{5+}$	–	4.10[a]
$H_5L^{5+} + F^- \rightleftharpoons [H_5LF]^{4+}$	–	3.20[a]
$H_6L^{6+} + Cl^- \rightleftharpoons [H_6LCl]^{5+}$	–	3.00[a], 2.26[b]
$H_5L^{5+} + Cl^- \rightleftharpoons [H_5LCl]^{4+}$	–	1.95[a], 1.71[b]
$H_4L^{4+} + Cl^- \rightleftharpoons [H_4LCl]^{3+}$	–	0.62[b]
$H_6L^{6+} + Br^- \rightleftharpoons [H_6LBr]^{5+}$	1.92[c]	2.60[a]
$H_5L^{5+} + Br^- \rightleftharpoons [H_5LBr]^{4+}$	1.89[c]	1.60[a]
$H_4L^{4+} + Br^- \rightleftharpoons [H_4LBr]^{3+}$	1.64[c]	–
$H_3L^{3+} + Br^- \rightleftharpoons [H_3LBr]^{2+}$	1.42[c]	–
$H_6L^{6+} + I^- \rightleftharpoons [H_6LI]^{5+}$	–	2.15[a]
$H_5L^{5+} + I^- \rightleftharpoons [H_5LI]^{4+}$	–	1.55[a]
$H_6L^{6+} + N_3^- \rightleftharpoons [H_6LN_3]^{5+}$	–	4.30[a]
$H_5L^{5+} + N_3^- \rightleftharpoons [H_5LN_3]^{4+}$	–	2.65[a]
$H_6L^{6+} + NO_3^- \rightleftharpoons [H_6LNO_3]^{5+}$	–	2.80[a], 2.93[b]
$H_5L^{5+} + NO_3^- \rightleftharpoons [H_5LNO_3]^{4+}$	–	1.65[a], 2.30[b]
$H_4L^{4+} + NO_3^- \rightleftharpoons [H_4LNO_3]^{3+}$	–	1.52[b]
$H_3L^{3+} + NO_3^- \rightleftharpoons [H_3LNO_3]^{2+}$	–	1.15[b]
$H_2L^{3+} + NO_3^- \rightleftharpoons [H_2LNO_3]^{+}$	–	0.50[b]

[a] I = 0.10 M NaTsO, Ref. [46].
[b] I = 0.10 M KCl, Ref. [45].
[c] I = 0.10 M KCl, Ref. [76].

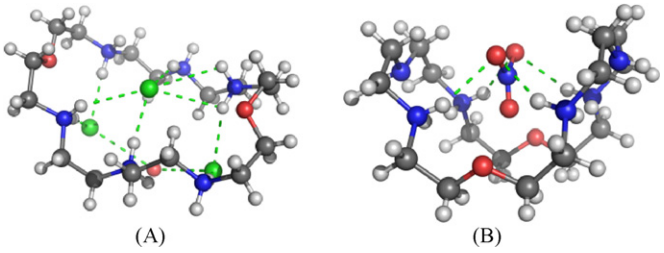

Fig. 9. Crystal structures of H_6**3m**·6Cl·4H_2O (A) [37] and [H_4**3m**NO_3]$^{3+}$ (B) [77].

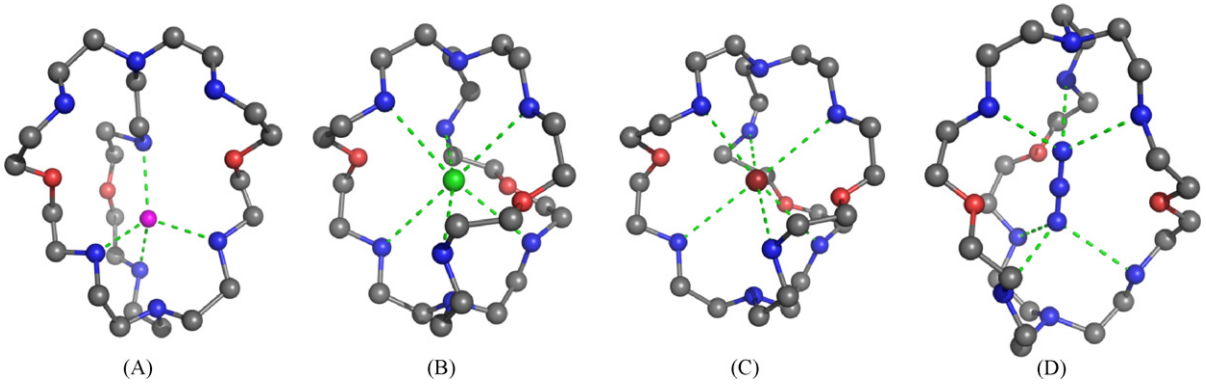

Fig. 10. X-ray structures of $H_6\mathbf{3c}^{6+}$ with F^- (A), Cl^- (B), Br^- (C) and N_3^- (D) [46,78].

[39,41,42,46,75,77,79]. With $H_n\mathbf{3m}^{n+}$ other anions were also studied that were not taken into account in this study for lack of the corresponding values with the cryptand, such as mesoxalate [40], acetohydroxamate [41], phosphite [43], selenite and selenate anions [76].

The anion binding is strongly dependent on electrostatic interactions between the negative oxygen atoms of the anions and the positive ammonium groups of the receptor, to which are also associated an extensive hydrogen-bonding formation N^+–H···$^-$O. The most stable associations were formed between the most charged species, ATP^{4-}, $P_2O_7^{4-}$ and ADP^{3-}, see diagrams of log K_{eff} in function of pH in Fig. 11a.

Unfortunately for $H_n\mathbf{3c}^{n+}$, association constants with only the hexa- and pentaprotonated forms of the receptor were reported in the early and unique report by Lehn and coworkers [46]. The lack of association constants for species with lower and higher number of protons leads to a deficient comparison with the macrocycle especially at low pH values. Nonetheless, as can be seen on Fig. 11, the difference in the magnitude of binding between the macrocycle and the cryptand for the polyphosphates and nucleotides is not very significant, which may be ascribed to the fact that these large substrates can only be partially included into the cavity of the cryptand. The $H_n\mathbf{3c}^{n+}$, however, presents the strongest binding interaction with $HP_2O_7^{3-}$ while in the case of the macrocycle the highest association is with $HATP^{3-}$ anion. Although this fact was not commented by the authors, it suggests a better accommodation of $HP_2O_7^{3-}$ into the cryptand cavity.

The binding of oxa^{2-} and mal^{2-} by $H_n\mathbf{3}^{n+}$ pair of receptors demonstrate better how the encapsulation of one anion by the cryptand results in enhanced selectivity [39,41]. As shown in Fig. 12a although the macrocycle is selective for oxa^{2-} in the presence of mal^{2-} at pH lower than 4, above pH 5 mal^{2-} is preferred. In fact, should mal^{2-} (completely deprotonated form) be able to coexist with the completely protonated form of the macrocycle it seems reasonable to assume that no discrimination would exist. The cryptand on the other hand, due to its structural features, is able to be hexaprotonated at the pH where both dicarboxylates are fully ionized, then showing a clear preference for oxalate throughout the whole pH range studied Fig. 12b.

While $H_n\mathbf{3m}^{n+}$ displays the largest K_{eff} values for all the anions at pH ≈ 4 (see Fig. 11a), it is at pH ≈ 6.5 the corresponding value for the cryptand (Fig. 11b) due to its capacity to be hexaprotonated at around this pH value. This is illustrated in Fig. 13, which shows that, below pH ≈ 4 sulfate is preferably bound to the macrocycle whereas above this value it is mostly bound by the cryptand.

In conclusion, the binding constants reveal that, for the series of mononegative anions, the $H_n\mathbf{3c}^{n+}$ cryptand shows topological discrimination, preferring the linear N_3^- to the spherical halides, although it is not selective. Due to its high charge density, and despite not occupying the cryptand cavity as well as Cl^-, Br^- and N_3^-, F^- has an association constant of the same magnitude of N_3^-. The lower than expected binding of the polyphosphates and nucleotides by $H_6\mathbf{3c}^{6+}$ relative to $H_6\mathbf{3m}^{6+}$ may be ascribed to the fact that these large substrates can only be partially included into

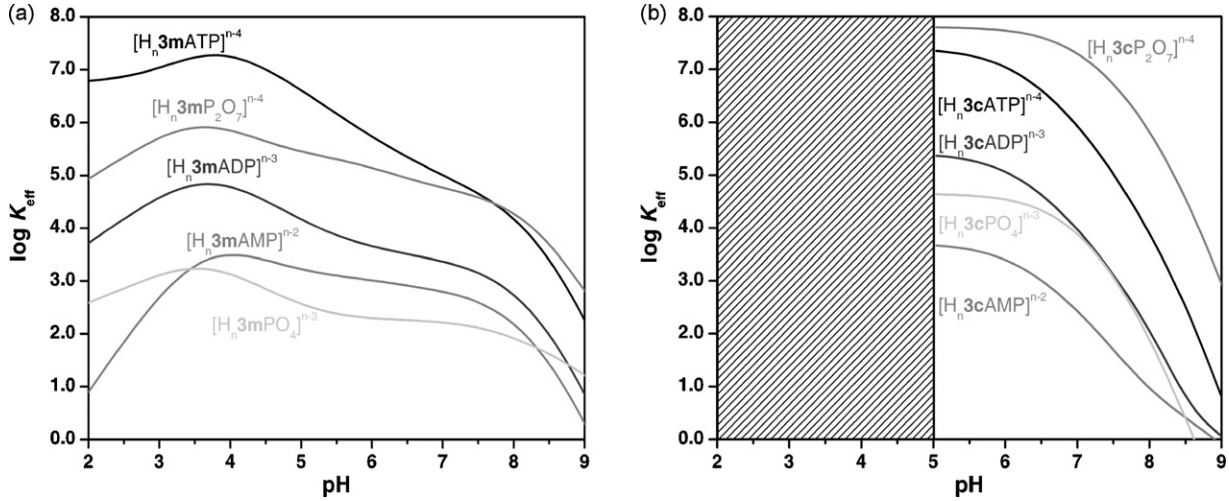

Fig. 11. Plots of the log K_{eff} *versus* pH for the associations formed between the indicated phosphate anions and $H_n\mathbf{3m}^{n+}$ (a) or $H_n\mathbf{3c}^{n+}$ (b). For the cryptand a restricted range of pH was considered due to lack of constants, see text.

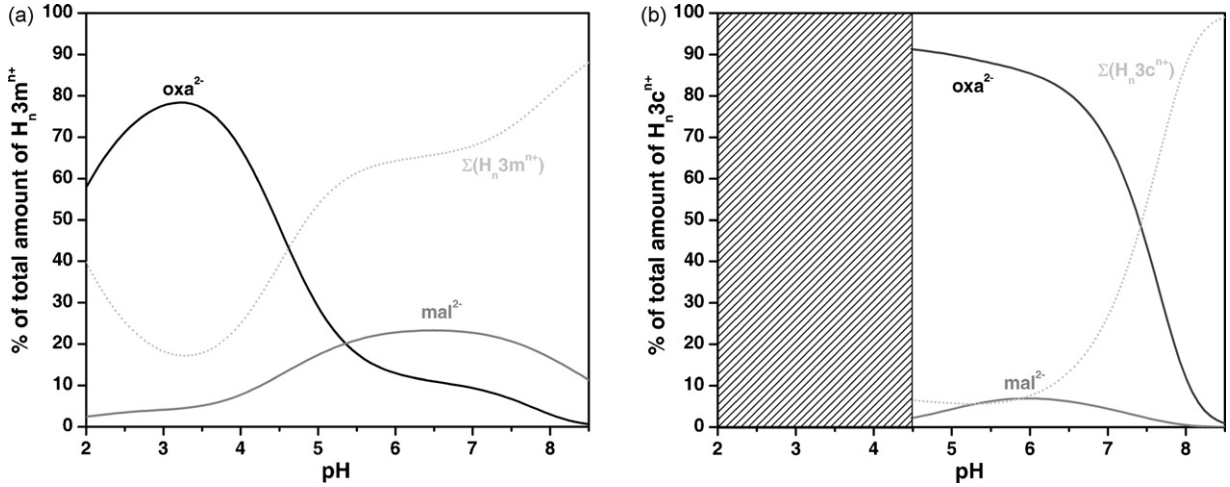

Fig. 12. Distribution diagrams of the overall amount of supramolecular species formed between H_n**3m**$^{n+}$, $H_n$oxa^{n-2} and $H_n$mal^{n-2} (a) and H_n**3c**$^{n+}$, $H_n$oxa^{n-2} and $H_n$mal^{n-2} (b). $C_{\mathbf{3m}} = C_{\mathbf{3c}} = C_{oxa} = C_{mal} = 2 \times 10^{-3}$ M. $I = 0.1$ M KCl, $T = 298.15$ K.

the cavity of the receptor. Probably the same happens in the comparison of oxa^{2-} and mal^{2-} [46].

On the other hand, the strong electrostatic interactions and extensive hydrogen bonding formed between H_n**3m**$^{n+}$ and ATP^{4-} instead to conduct to inert supramolecular compounds increases the reactivity of the phosphorus centre towards nucleophilic agents, resulting in hydrolysis of the triphosphate linkage. The hydrolysis of the nucleotides results from an initial nucleophilic attack on the nucleotide by the electron donor supplied by the solvent water, or by an unprotonated nitrogen of the macrocycle or other catalytic molecule. The nucleophile attacks the phosphorus centre of the nucleotide ATP to form ADP and an intermediate phosphoramide [80–82].

3.4. Macrocycle ***4m*** and cryptand ***4c***

Interaction studies between monocharged anions and the H_n**4m**$^{n+}$ macrocyclic receptor are not reported. However the binding of H_n**4m**$^{n+}$ with dicarboxylate (oxa^{2-}, mal^{2-}), mono-, di- and triphosphate [47,83], and nucleotide anions (AMP^{2-}, ADP^{3-}, ATP^{4-}) [84] in aqueous solution was investigated, see Table 15 [47,83,84] and Fig. 14. The strength of the binding between H_n**4m**$^{n+}$ and the anions increases in the order $HPO_4^{2-} < P_2O_7^{4-} < P_3O_{10}^{5-}$ and AMP^{2-} < ADP^{3-} < ATP^{4-} (Fig. 14), corresponding to the increase in the number of hydrogen bonds and coulombic attractive forces. Molecular catalysis of ATP-hydrolysis by H_n**4m**$^{n+}$ has also been observed at low pH and the mechanism of the reaction proposed. In this case, a pentacovalent oxyphosphorane intermediate is formed, followed by the cleavage of the P(α) group of ATP [84].

Crystal structures of the associations with mono-, di- and triphosphate were reported [47,83]. The crystal structure of $[H_6$**4m**$(H_2PO_4)]HPO_4 3Br \cdot 3.5H_2O$ shows that the dihydrogen phosphate is bound through three medium to strong hydrogen bonds (2.67–2.77 Å). The macrocycle adopts a boat conformation with the two furan rings approximately parallel to each other and with both furan-oxygen atoms pointing to the same side of the plane defined by the six nitrogen atoms [83]. The $H_2PO_4^-$ anion is located above the ellipsoid plane and is sandwiched between two aromatic rings. The crystal structure of $[H_5$**4m**$(H_2P_2O_7)]^{3+}$ (Fig. 15) reveals that the anion is inserted into the macrocycle forming a pseudo-rotaxane

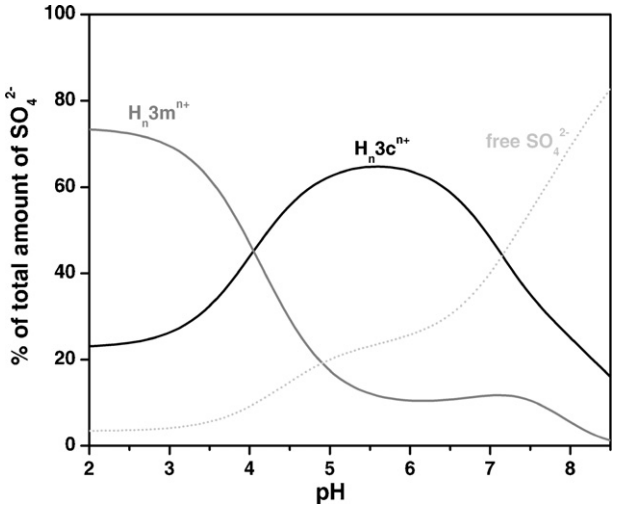

Fig. 13. Distribution diagram of the overall amount of supramolecular species formed between H_n**3m**$^{n+}$ and H_n**3c**$^{n+}$ and sulfate. $C_{\mathbf{3m}} = C_{\mathbf{3c}} = C_{sulfate} = 2 \times 10^{-3}$ M. $I = 0.1$ M KCl, $T = 298.15$ K.

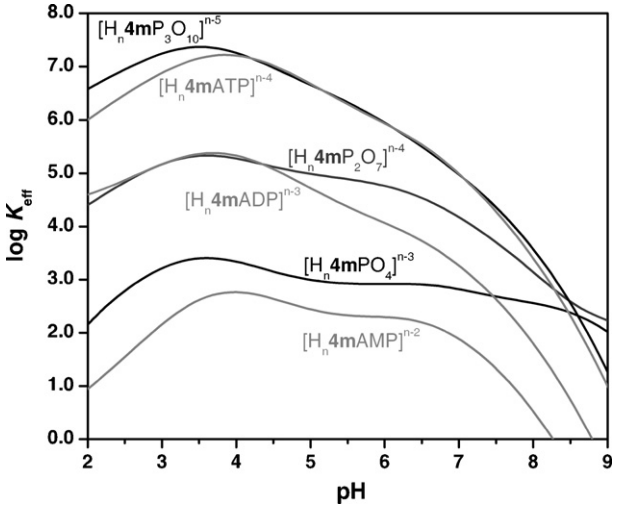

Fig. 14. Plots of the effective association constant ($\log K_{eff}$) *versus* pH for the supramolecular species formed between H_n**4m**$^{n+}$ and the indicated anions. $C_{\mathbf{4m}} = C_A = 2 \times 10^{-3}$ M [47,83,84].

Table 14
Stepwise association constants ($\log K_{H_hL_lA_a}$) for the indicated equilibrium in aqueous solution; T = 298.15 K.

Equilibrium	$\log K_{H_hL_lA_a}$	
	L = **3m**	L = **3c**
$H_6L^{6+} + SO_4^{2-} \rightleftharpoons [H_6LSO_4]^{4+}$	4.61[a]	4.90[b], 3.63[a]
$H_5L^{5+} + SO_4^{2-} \rightleftharpoons [H_5LSO_4]^{3+}$	3.68[a]	2.90[b], 2.72[a]
$H_4L^{4+} + SO_4^{2-} \rightleftharpoons [H_4LSO_4]^{2+}$	2.31[a]	2.60[a]
$H_3L^{3+} + SO_4^{2-} \rightleftharpoons [H_3LSO_4]^{+}$	–	2.25[a]
$H_2L^{2+} + SO_4^{2-} \rightleftharpoons [H_2LSO_4]$	–	1.78[a]
$H_6L^{6+} + oxa^{2-} \rightleftharpoons [H_6Loxa]^{4+}$	4.68[c]	4.95[b]
$H_5L^{5+} + oxa^{2-} \rightleftharpoons [H_5Loxa]^{3+}$	3.59[c]	3.35[b]
$H_4L^{4+} + oxa^{2-} \rightleftharpoons [H_4Loxa]^{2+}$	2.06[c]	–
$H_6L^{6+} + Hmal^{-} \rightleftharpoons [H_7Lmal]^{5+}$	2.2[d]	–
$H_6L^{6+} + mal^{2-} \rightleftharpoons [H_6Lmal]^{4+}$	4.2[d] (2.23*)	3.10[b]
$H_5L^{5+} + mal^{2-} \rightleftharpoons [H_5Lmal]^{3+}$	3.70[d] (2.25*)	2.00[b]
$H_4L^{4+} + mal^{2-} \rightleftharpoons [H_4Lmal]^{2+}$	2.38[d]	–
$H_3L^{3+} + mal^{2-} \rightleftharpoons [H_3Lmal]^{+}$	2.05[d]	–
$H_2L^{2+} + mal^{2-} \rightleftharpoons [H_2Lmal]$	1.81[d]	–
$H_6L^{6+} + H_2PO_4^{-} \rightleftharpoons [H_8LPO_4]^{5+}$	2.66[d]	–
$H_6L^{6+} + HPO_4^{2-} \rightleftharpoons [H_7LPO_4]^{4+}$	6.97[d] (3.52*)	5.50[b] (4.65*)
$H_5L^{5+} + HPO_4^{2-} \rightleftharpoons [H_6LPO_4]^{3+}$	5.2[d] (2.27*)	2.75[b]
$H_4L^{4+} + HPO_4^{-} \rightleftharpoons [H_5LPO_4]^{2+}$	2.6[d]	–
$H_3L^{3+} + HPO_4^{2-} \rightleftharpoons [H_4LPO_4]^{+}$	1.85[d]	–
$H_2L^{2+} + HPO_4^{2-} \rightleftharpoons [H_3LPO_4]$	1.49[d]	–
$H_6L^{6+} + H_2P_2O_7^{2-} \rightleftharpoons [H_8LP_2O_7]^{4+}$	4.86[e]	–
$H_6L^{6+} + HP_2O_7^{3-} \rightleftharpoons [H_7LP_2O_7]^{3+}$	8.80[e] (6.22*)	–
$H_6L^{6+} + P_2O_7^{4-} \rightleftharpoons [H_6LP_2O_7]^{2+}$	12.56[e] (5.36*)	10.30[b] (7.8*)
$H_5L^{5+} + P_2O_7^{4-} \rightleftharpoons [H_5LP_2O_7]^{+}$	9.35[e] (4.74*)	6.45[b] (5.05*)
$H_4L^{4+} + P_2O_7^{4-} \rightleftharpoons [H_4LP_2O_7]$	5.21[e] (4.44*)	–
$H_3L^{3+} + P_2O_7^{4-} \rightleftharpoons [H_3LP_2O_7]^{-}$	3.44[e] (3.31*)	–
$H_2L^{2+} + P_2O_7^{4-} \rightleftharpoons [H_2LP_2O_7]^{2-}$	2.41[e]	–
$HL^{+} + P_2O_7^{4-} \rightleftharpoons [HLP_2O_7]^{3-}$	2.08[e]	–
$H_6L^{6+} + AMP^{2-} \rightleftharpoons [H_6LAMP]^{4+}$	6.95[f] (4.10*)	3.85[b] (3.54*)
$H_5L^{5+} + AMP^{2-} \rightleftharpoons [H_5LAMP]^{3+}$	5.50[f] (3.08*)	2.65[b]
$H_4L^{4+} + AMP^{2-} \rightleftharpoons [H_4LAMP]^{2+}$	2.85[f]	–
$H_6L^{6+} + HADP^{2-} \rightleftharpoons [H_7LADP]^{4+}$	5.60[f] (5.08*)	
$H_6L^{6+} + ADP^{3-} \rightleftharpoons [H_6LADP]^{3+}$	8.30[f] (5.31*)	5.85[b] (5.40*)
$H_5L^{5+} + ADP^{3-} \rightleftharpoons [H_5LADP]^{2+}$	6.20[f] (3.64*)	4.15[b] (4.80*)
$H_4L^{4+} + ADP^{3-} \rightleftharpoons [H_4LADP]^{+}$	3.40[f]	–
$H_6L^{6+} + H_2ATP^{2-} \rightleftharpoons [H_8LATP]^{4+}$	6.75[f]	–
$H_6L^{6+} + HATP^{3-} \rightleftharpoons [H_7LATP]^{3+}$	7.85[f] (7.31*)	–
$H_6L^{6+} + ATP^{4-} \rightleftharpoons [H_6LATP]^{2+}$	11.00[f] (7.86*)	8.00[b] (7.40*)
$H_5L^{5+} + ATP^{4-} \rightleftharpoons [H_5LATP]^{+}$	8.15[f] (5.44*)	5.40[b] (5.90*)
$H_4L^{4+} + ATP^{4-} \rightleftharpoons [H_4LATP]$	4.80[f]	–

[a] I = 0.1 M KCl, Ref. [79].
[b] I = 0.1 M NaTsO, Ref. [46].
[c] I = 0.1 M KCl, Ref. [39].
[d] I = 0.1 M KCl, Ref. [41].
[e] I = 0.1 M KCl, Ref. [42].
[f] I = 0.1M NaTsO, Ref. [75].
* Value in agreement with the K_{eff} *versus* pH diagram, indicating that for this value the correct equilibrium was not ascribed by the authors; instead the correct one is established between a species having one less proton in the receptor and one proton more in the anion. For instance, the correct equilibrium is $H_5\mathbf{3m}^{5+} + H_2P_2O_7^{2-} \rightleftharpoons [H_7\mathbf{3m}P_2O_7]^{3+}$ instead of $H_6\mathbf{3m}^{6+} + HP_2O_7^{3-} \rightleftharpoons [H_7\mathbf{3m}P_2O_7]^{3+}$, as can be seen in Fig. 11a at pH about 3.5 the maximum log K_{eff} is about 6.

molecule, held by four weak to strong hydrogen bonds with N···O distances ranging 2.64–2.81 Å. Additionally, there is a longer hydrogen bond (2.98 Å) which the authors proposed to be formed between one of the $H_2P_2O_7^{2-}$ OH groups and one deprotonated

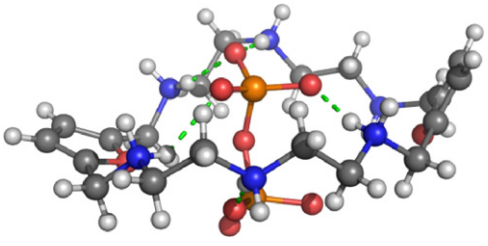

Fig. 15. Crystal structure of the association of $H_6\mathbf{4m}^{6+}$ and pyrophosphate [47].

Table 15
Stepwise association constants ($\log K_{H_hL_lA_a}$) for the indicated equilibrium in aqueous solution, T = 298.15 K[a].

Equilibrium[a]	$\log K_{L_lH_hA_a}$	
	L = **4m**	L = **4c**
$H_6L^{6+} + NO_3^{-} \rightleftharpoons [H_6LNO_3]^{5+}$	–	3.35[a], [3.63][a,b]
$H_6L^{6+} + ClO_4^{-} \rightleftharpoons [H_6LClO_4]^{5+}$	–	2.29[a], [2.66][a,b]
$H_6L^{6+} + SO_4^{2-} \rightleftharpoons [H_6LSO_4]^{4+}$	–	7.21[c]
$H_5L^{5+} + SO_4^{2-} \rightleftharpoons [H_5LSO_4]^{3+}$	–	5.21[c]
$H_4L^{4+} + SO_4^{2-} \rightleftharpoons [H_4LSO_4]^{2+}$	–	4.32[c]
$H_3L^{3+} + SO_4^{2-} \rightleftharpoons [H_3LSO_4]^{+}$	–	4.02[c]
$H_2L^{2+} + SO_4^{2-} \rightleftharpoons [H_2LSO_4]$	–	3.37[c]
$H_6L^{6+} + Hoxa^{-} \rightleftharpoons [H_7Loxa]^{5+}$	–	7.17[d]
$H_6L^{6+} + oxa^{2-} \rightleftharpoons [H_6Loxa]^{4+}$	4.97[e] (4.29*)	8.30[d]
$H_5L^{5+} + oxa^{2-} \rightleftharpoons [H_5Loxa]^{3+}$	4.12[e]	7.12[d]
$H_4L^{4+} + oxa^{2-} \rightleftharpoons [H_4Loxa]^{2+}$	2.97[e]	5.53[d]
$H_3L^{2+} + oxa^{2-} \rightleftharpoons [H_3Loxa]^{+}$	–	4.82[d]
$H_2L^{2+} + oxa^{2-} \rightleftharpoons [H_2Loxa]$	–	4.05[d]
$H_6L^{6+} + Hmal^{-} \rightleftharpoons [H_7Lmal]^{5+}$	1.86[e]	5.64[d]
$H_6L^{6+} + mal^{2-} \rightleftharpoons [H_6Lmal]^{4+}$	4.01[e] (1.90*)	6.62[d]
$H_5L^{5+} + mal^{2-} \rightleftharpoons [H_5Lmal]^{3+}$	3.39[e] (1.94*)	5.55[d]
$H_4L^{4+} + mal^{2-} \rightleftharpoons [H_4Lmal]^{2+}$	2.10[e]	5.00[d]
$H_3L^{3+} + mal^{2-} \rightleftharpoons [H_3Lmal]^{+}$	–	4.42[d]
$H_2L^{2+} + mal^{2-} \rightleftharpoons [H_2Lmal]$	–	3.62[d]
$H_6L^{6+} + ac^{-} \rightleftharpoons [H_6Lac]^{5+}$	–	3.73[d]
$H_5L^{5+} + ac^{-} \rightleftharpoons [H_5Lac]^{4+}$	–	3.99[d]
$H_4L^{4+} + ac^{-} \rightleftharpoons [H_4Lac]^{3+}$	–	4.01[d]
$H_3L^{3+} + ac^{-} \rightleftharpoons [H_3Lac]^{2+}$	–	3.93[d]
$H_2L^{2+} + ac^{-} \rightleftharpoons [H_2Lac]^{+}$	–	3.43[d]
$H_6L^{6+} + lac^{-} \rightleftharpoons [H_6Llac]^{5+}$	–	3.50[d]
$H_5L^{5+} + lac^{-} \rightleftharpoons [H_5Llac]^{4+}$	–	3.75[d]
$H_4L^{4+} + lac^{-} \rightleftharpoons [H_4Llac]^{3+}$	–	3.30[d]
$H_3L^{3+} + lac^{-} \rightleftharpoons [H_3Llac]^{2+}$	–	3.13[d]
$H_2L^{2+} + lac^{-} \rightleftharpoons [H_2Llac]^{+}$	–	2.91[d]

[a] I = 0.1 M NaTsO, Ref. [52].
[b] In brackets values obtained by NMR titration data.
[c] I = 0.1 M NaTsO, Ref. [85].
[d] I = 0.1 M in NaTsO, Ref. [48].
[e] I = 0.1 M in KCl, Ref. [47].
* Value in agreement with the K_{eff} *versus* pH diagram, indicating that for this value the correct equilibrium was not ascribed by the authors; instead the correct one is established between a species having one less proton in the receptor and one more proton in the anion.

nitrogen atom of the macrocycle. Interestingly at pH 3.5, where this species is the major one in solution, the log K_{eff} *versus* pH curve reaches a maximum (Fig. 14), indicating that this is the most stable species [47]. In the crystal structure of the association with triphosphate there are two asymmetric units present in the unit cell which contains two $[H_n\mathbf{4m}(H_nP_3O_{10})]^{n-5}$, one $[H_n\mathbf{4m}(H_nP_3O_{10})_2]^{n-10}$, one chloride anion and 40 water molecules. The location and total number of the hydrogen atoms was not specified by the authors. In the structure of $[H_n\mathbf{4m}H_nP_3O_{10}]^{n-5}$, seven of the eight terminal oxygen atoms of triphosphate form hydrogen bonds to the nitrogen atoms of the macrocycle. One of the terminal phosphate groups and the central one are included in the macrocyclic cavity similarly to what was observed for diphosphate and the third phosphate group is positioned in a way that two terminal oxygen atoms are located above the macrocyclic cavity close to one end of the macrocycle forming hydrogen bonds. A total of nine hydrogen bonds are formed in this association, demonstrating very strong interaction between the macrocycle and triphosphate. The hydrogen bond distances range from 2.67 to 2.98 Å. In the structure of $[H_n\mathbf{4m}(H_nP_3O_{10})_2]^{n-10}$ two triphosphate anions bind to the same protonated macrocycle, with one above and the other below the cavity plane. Each triphosphate anion uses three terminal oxygen atoms to form four hydrogen bonds with one diethylenetriamine unit and one oxygen atom to form two hydrogen bonds with the second diethylenetriamine unit. The hydrogen bond distances range from 2.69 to 2.92 Å [83]. These crystal structures support the results obtained from solution studies.

Potentiometric data indicate also that H_n**4m**$^{n+}$ shows a preference for oxalate over malonate anions [47]. The effect of structural match between the receptor and substrate prevails over the basicity of the anion, and the binding of flexible mal^{2-} anion by H_n**4m**$^{n+}$ is weaker than that of rigid oxa^{2-} anion, see Table 15.

Crystal structures only exist for the association with oxalate, which is shown in Fig. 16 [47]. The oxa^{2-} anions are located above and below the macrocyclic plane, each anion binds to H_6**4m**$^{6+}$ through six hydrogen bonds. One of the oxygen atoms from one of the carboxylates forms two hydrogen bonds simultaneously with the two central nitrogen atoms of one receptor (2.65 and 2.83 Å), while the second oxygen atom of each carboxylate forms a hydrogen bond with one of the central nitrogen atoms of a diethylenetriamine unit (2.75 Å). The remaining two oxygen atoms of the oxa^{2-} anion are also hydrogen-bonded to another protonated macrocyclic ligand with the same pattern of bonds. The $-N^+-H\cdots{}^-O$ distances correspond to strong hydrogen bonds.

Nelson and coworkers investigated the binding interactions of the H_n**4c**$^{n+}$ cryptand with different oxoanions showing a charge and shape-based selectivity behavior in aqueous solution [48,52,85–88]. The binding constants of carboxylates, such as ac^-, lac^-, oxa^{2-} and mal^{2-}, with H_n**4c**$^{n+}$ are markedly higher for dinegative anions, testifying again the dominance of electrostatic interactions. Moreover, carboxylates differ from other oxoanions in many respects, such as geometry and higher basicity, thus, the affinity of ac^- and lac^- for H_n**4c**$^{n+}$ is higher than NO_3^- and ClO_4^- [48,52].

An exceptional high log K value of 8.30 was found for the formation of [H_6**4c**(oxa)]$^{4+}$ [48]. The crystal structure of [H_6**4c**(oxa)]$^{4+}$ [87], illustrated in Fig. 17, shows the oxa^{2-} anion completely encapsulated into the receptor cavity forming six moderately strong hydrogen bonds (with distances in the range of 2.76–3.04 Å) *via* only one oxygen of each carboxylate group. Moreover, one end of the oxalate anion is sandwiched between two of the aromatic π-systems forming a triple π-stacking interaction, and the other end is also interacting with the last aromatic ring. This suggests that in crystal exists a very good accommodation of oxalate within the cavity of H_6**4c**$^{6+}$.

Crystal structures of three other oxoanions of particular environmental/biological significance, CrO_4^{2-}, SeO_4^{2-} and $S_2O_3^{2-}$, with the anion encapsulated into the cavity were also reported [86]. The dinegative anions invariably occupy the cavity of H_n**4c**$^{n+}$, establishing a network of hydrogen bonds, in agreement with solution studies that demonstrated a special selectivity for these dinegative anions over the mononegative analogues.

Oxalate and malonate anions are selectively recognized by the H_n**4c**$^{n+}$ in presence of an equimolar amount of the H_n**4m**$^{n+}$ on the entire pH scale, see Fig. 18. The authors suggest that the exceptionally large association constant of the oxalate anion by H_n**4c**$^{n+}$ can be partly explained by multiple π-stacking interactions described above [48,87]. Additionally, this especial interaction comes also from the capability of the macrobicycle to encapsulate specific anions, depending of shape, size, number and position of the binding sites [48,87]. These results indicate that the dicarboxylate binding is not governed only by electrostatic interactions but also the geometrical fit of the anion into the receptor play a crucial role.

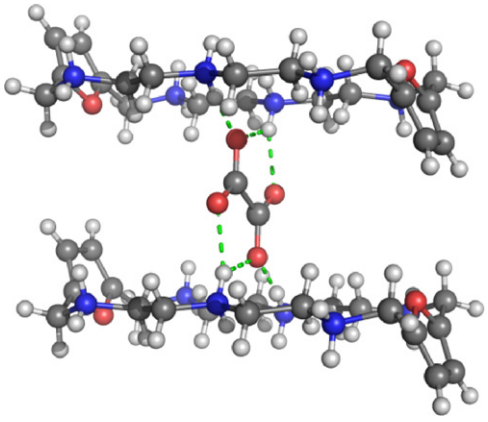

Fig. 16. Crystal structure of the association between H_6**4m**$^{6+}$ and oxa^{2-} anion [47].

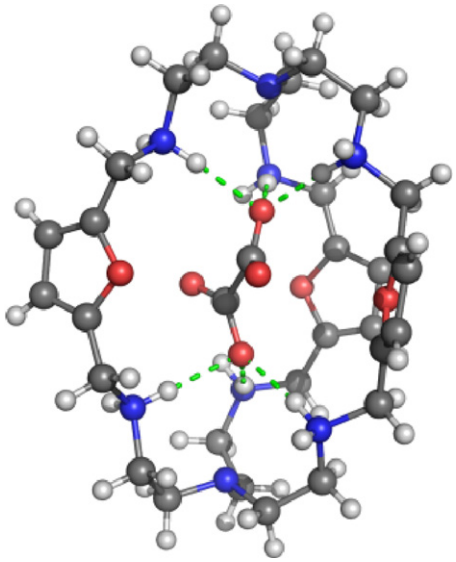

Fig. 17. Crystal structure of the supermolecule formed between H_6**4c**$^{6+}$ and oxalate anion [87].

3.5. Macrocycle ***5m*** and cryptand ***5c***

There are no binding constant values for the association of Cl^-, Br^-, NO_3^- and ClO_4^- by H_n**5m**$^{n+}$ reported, however some assumptions are possible with the available information. For instance, it was found that the association constant for nitrate is less than 2 log units [89], and that the protonation constants of the macrocycle in 0.1 M KNO_3 are not changed by the presence of up to 4 equiv. of KBr [90]. Furthermore, the similarity of the protonation constants obtained in KNO_3 [91], KCl [92] and $NaClO_4$ [50] media (Table 16) suggests that there is no preferential binding of any of these anions by the macrocycle. These results indicate that the association constants of H_6**5m**$^{6+}$ with Cl^-, Br^-, NO_3^- and ClO_4^- are all <2 log units.

Crystal structures of H_6**5m**$^{6+}$ with Br^- and NO_3^- are in agreement with these findings (Fig. 19). In the former crystal structure two of six Br^- anions are bound closer to the centre of the macrocycle above and below the plane formed by the six nitrogen atoms. Each Br^- anions are only bound by two hydrogen bonds (average $Br\cdots N$ distance of 3.32 Å) with two adjacent nitrogen atoms of each

Table 16
Stepwise protonation (K_i^H) constants of **5m** in aqueous solution; T = 298.15 K.

Equilibrium	log K_i^H				
5m + H^+ ⇌ H**5m**$^+$	9.49[a]	9.58[b]	9.51[c]	9.49[d]	9.72[e]
H**5m**$^+$ + H^+ ⇌ H_2**5m**$^{2+}$	8.73[a]	8.79[b]	8.77[c]	8.77[d]	8.96[e]
H_2**5m**$^{2+}$ + H^+ ⇌ H_3**5m**$^{3+}$	8.03[a]	8.08[b]	7.97[c]	8.04[d]	8.23[e]
H_3**5m**$^{3+}$ + H^+ ⇌ H_4**5m**$^{4+}$	7.29[a]	7.34[b]	7.09[c]	7.18[d]	7.51[e]
H_4**5m**$^{4+}$ + H^+ ⇌ H_5**5m**$^{5+}$	3.64[a]	3.70[b]	3.79[c]	3.51[d]	4.50[e]
H_5**5m**$^{5+}$ + H^+ ⇌ H_6**5m**$^{6+}$	3.45[a]	3.37[b]	3.27[c]	3.09[d]	3.50[e]

[a] I = 0.1 M in KNO_3, Ref. [91].
[b] I = 0.1 M in KNO_3, Ref. [90].
[c] I = 0.1 M in KCl, Ref. [92].
[d] I = 0.1 M in $NaClO_4$, Ref. [50].
[e] I = 0.1 M in NaTsO, Ref. [51].

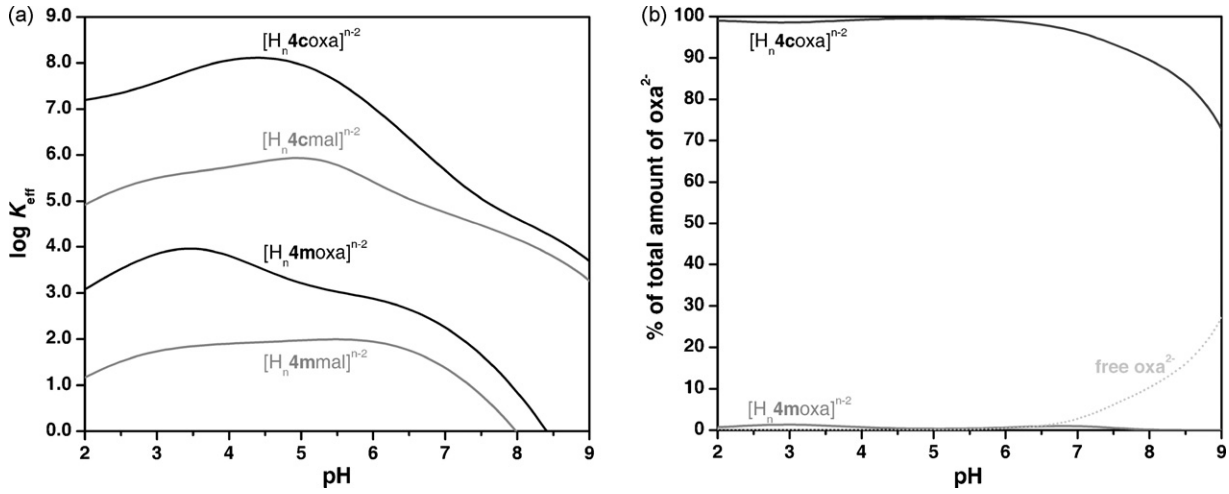

Fig. 18. Plot of the effective association constant (log K_{eff}) *versus* pH for the supramolecular species formed between H_n**4m**$^{n+}$ and H_n**4c**$^{n+}$ and the indicated anions (a), and distribution diagram of the overall amounts of supramolecular species formed by oxa^{2-} with H_n**4m**$^{n+}$ and H_n**4c**$^{n+}$ receptors in equimolar ratio (b). $C_{\mathbf{4m}} = C_{\mathbf{4c}} = C_A = 2 \times 10^{-3}$ M [47,48].

diethylenetriamine unit facing the interior of the macrocycle [92]. The crystal structure with NO_3^- is similar in the sense that the macrocycle has a relatively planar ellipsoid geometry. However in this case only the two central amines are involved in hydrogen bonding with nitrate ($O_{nitrate}\cdots N$ of 2.829 and 2.779 Å), which is located above the plane defined by the six N atoms. The rest of the ammonium groups are pointing to the outside of the cavity and involved in hydrogen bonding with other nitrate anions from the outside [89]. This structural information suggests that bromide and nitrate should be loosely bound to H_6**5m**$^{6+}$.

Sulfate was found to be strongly bound by H_6**5m**$^{6+}$ with an association constant of 4.36 log units in tosylate medium. The presence of chloride lowers the association constant as expected, $\log K_{[H_6\mathbf{5m}SO_4]} = 4.07$ in 0.1 M KCl, see Table 17 [89]. The crystal structure of the binding of sulfate by H_6**5m**$^{6+}$ shows the macrocycle in relatively planar ellipsoid geometry with only the two central amines of each diethylenetriamine unit involved in hydrogen bonding with sulfate ($O_{sulfate}\cdots N$ distance of 2.686 Å) and the rest of the ammonium groups are pointing to the outside of the cavity. This crystal structure is almost identical to that of nitrate, with one sulfate anion taken in sandwich between two macrocycles (Fig. 20A).

The $H_2PO_4^-$ is bound to H_5**5m**$^{5+}$ with an association constant of 3.86*, value comparable with that of sulfate [92], indicating that electrostatic interactions may not be the only factor involved. It was found for instance that $H_2P_2O_7^{2-}$ (unlike Br^-, NO_3^- and SO_4^{2-}) is positioned inside the H_4**5m**$^{4+}$ macrocyclic cavity (Fig. 20B) [92]. In this case, the H_4**5m**$^{4+}$ adopts a bowl conformation instead of the chair configuration, in order to include the $H_2P_2O_7^{2-}$ anion in its cavity. Note that although this dinegative anion is interacting with a less protonated form of the macrocycle, the association constant is 5.58 log units, 1.57 log units more than that of SO_4^{2-} interacting with the H_6**5m**$^{6+}$ in the same medium. This clearly shows that fac-

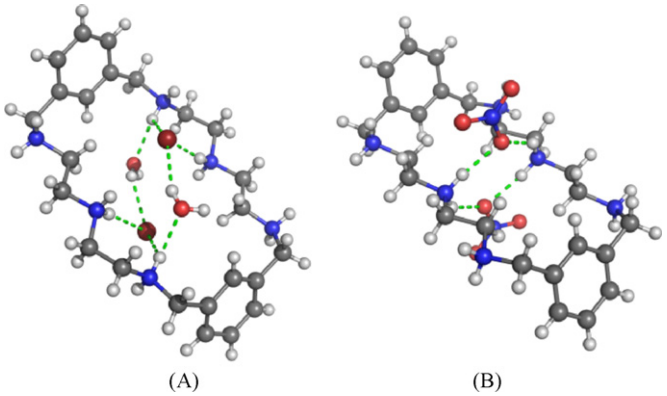

Fig. 19. X-ray crystal structure of the associations of H_6**5m**$^{6+}$ with bromide [92] and nitrate [8].

Table 17
Stepwise (log $K_{H_hL_lA_a}$) association constants for the indicated equilibria in aqueous solution; T = 298.15 K.

Equilibrium[a]	log $K_{H_hL_lA_a}$	
	L = **5m**	L = **5c**
$H_7L^{7+} + HF \rightleftharpoons [H_8LF]^{7+}$	–	3.53[a]
$H_7L^{7+} + F^- \rightleftharpoons [H_7LF]^{6+}$	–	4.29[a]
$H_6L^{6+} + F^- \rightleftharpoons [H_6LF]^{5+}$	[~2][a]	3.56[a], [3.64][a,b]
$H_5L^{5+} + F^- \rightleftharpoons [H_5LF]^{4+}$	–	3.20[a]
$H_4L^{4+} + F^- \rightleftharpoons [H_4LF]^{3+}$	–	2.49[a]
$H_3L^{3+} + F^- \rightleftharpoons [H_3LF]^{2+}$	–	2.06[a]
$H_2L^{2+} + F^- \rightleftharpoons [H_2LF]^{+}$	–	2.29[a]
$H_6L^{6+} + ClO_4^- \rightleftharpoons [H_6LClO_4]^{5+}$	–	3.25[c], [3.53][b,c]
$H_7L^{7+} + NO_3^- \rightleftharpoons [H_7LNO_3]^{6+}$	–	3.55[d], [3.69][b,d]
$H_6L^{6+} + NO_3^- \rightleftharpoons [H_6LNO_3]^{5+}$	<2[d]	3.02[e], 3.73[c], [3.74][b,c], 3.11[d]
$H_7L^{7+} + SO_4^{2-} \rightleftharpoons [H_7LSO_4]^{5+}$	–	4.97[d]
$H_6L^{6+} + SO_4^{2-} \rightleftharpoons [H_6LSO_4]^{4+}$	4.36[d], 4.07[f]	4.43[d], 6.57[g]
$H_5L^{5+} + SO_4^{2-} \rightleftharpoons [H_5LSO_4]^{3+}$	3.53[d], 3.04[f]	4.72[g]
$H_4L^{4+} + SO_4^{2-} \rightleftharpoons [H_4LSO_4]^{2+}$	–	3.70[g]
$H_3L^{3+} + SO_4^{2-} \rightleftharpoons [H_3LSO_4]^{+}$	–	3.47[g]
$H_2L^{2+} + SO_4^{2-} \rightleftharpoons [H_2LSO_4]$	–	3.06[g]
$H_6L^{6+} + Hoxa^- \rightleftharpoons [H_7Loxa]^{5+}$	–	13.83[h]
$H_6L^{6+} + oxa^{2-} \rightleftharpoons [H_6Loxa]^{4+}$	5.83[i]	10.71[h]
$H_5L^{5+} + oxa^{2-} \rightleftharpoons [H_5Loxa]^{3+}$	4.76[i]	8.64[h]
$H_4L^{4+} + oxa^{2-} \rightleftharpoons [H_4Loxa]^{2+}$	3.33[i]	7.15[h]
$H_3L^{3+} + oxa^{2-} \rightleftharpoons [H_3Loxa]^{+}$	2.50[i]	5.40[h]
$H_2L^{2+} + oxa^{2-} \rightleftharpoons [H_2Loxa]$	2.18[i]	–
$H_6L^{6+} + Hmal^- \rightleftharpoons [H_7Lmal]^{5+}$	–	5.77[h]
$H_6L^{6+} + mal^{2-} \rightleftharpoons [H_6Lmal]^{4+}$	–	7.22[h]
$H_5L^{5+} + mal^{2-} \rightleftharpoons [H_5Lmal]^{3+}$	–	6.20[h]
$H_4L^{4+} + mal^{2-} \rightleftharpoons [H_4Lmal]^{2+}$	–	5.79[h]
$H_3L^{3+} + mal^{2-} \rightleftharpoons [H_3Lmal]^{+}$	–	4.87[h]

[a] I = 0.1 M NaTsO, Ref. [51].
[b] Values in brackets correspond to NMR titration data.
[c] I = 0.1 M NaTsO, Ref. [52].
[d] I = 0.1 M NaTsO, Ref. [89].
[e] I = 0.1 M NaTsO, Ref. [96].
[f] I = 0.1 M KCl, Ref. [89].
[g] I = 0.1 M NaTsO, Ref. [85].
[h] I = 0.1 M NaTsO, Ref. [48].
[i] I = 0.1 M KCl, Ref. [54].

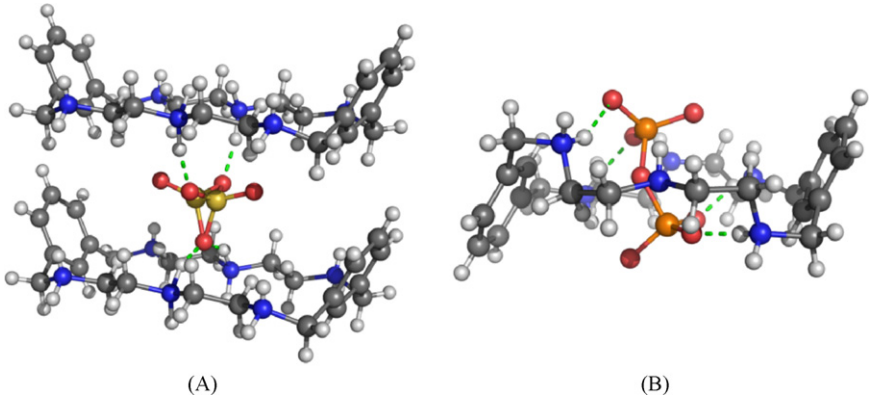

Fig. 20. Crystal structures of the association of sulfate by H_6**5m**$^{6+}$ (A) [89], and of the pseudo-rotaxane formed by H_4**5m**$^{4+}$ and dihydrogen pyrophosphate (B) [92]. In (A) the sulfate directly above the centre of one macrocycle exhibits 0.5 occupancy with its disordered counterpart (both disordered sulfate anions are shown) [89].

tors other than just charge govern the binding in these systems, as already discussed in Section 3.1.

It was also found that H_n**5m**$^{n+}$ binds strongly the di- and triphosphates [92] and nucleotides [93] by taking advantage of electrostatic interactions and hydrogen bonds, see Fig. 21. It has to be pointed out that the authors reported very high values for the stepwise association constants of H_n**5m**$^{n+}$ with these anions due to the incorrect assignment of the respective equilibria. For instance, as shown in Fig. 21, the K_{eff} for the ATP binding never gets higher than 7.25 log units, which means that no stepwise association constant much higher than this value should exist, thus the reported value of 11.15 log units for the equilibrium $H_5L^{5+} + HATP^{3-} \rightleftharpoons [H_6LATP]^{2+}$, which would be present at pH 4.5, is clearly not correct.

Several crystal structures of the H_n**5c**$^{n+}$ cryptand with several halide anions were reported. The crystal structure of the association of H_8**5c**$^{8+}$ with bromide revealed no encapsulation of Br^- but instead three bromide anions where found binding in a cleft manner [53], while encapsulation of fluoride and a water molecule by H_6**5c**$^{6+}$ was found by Bowman-James and coworkers [94]. The internal F^- and H_2O molecule were found to be shifted from the C_3 axis between the two apical nitrogen atoms of the receptor, with F^- bound *via* hydrogen bonds with three ammonium hydrogen atoms as well as with one hydrogen belonging to the internal water molecule, forming a pseudotetrahedral geometry. In addition, F^- encapsulation by the cryptand has been further substantiated by ^{19}F NMR techniques in H_2O/DMSO (60:40, v/v) solutions at 248.15 K. NMR and potentiometric titrations revealed that H_6**5c**$^{6+}$ binds fluoride stronger than does H_6**5m**$^{6+}$ by about 1.5 log units (Table 17). Recently a crystal structure revealed the encapsulation of iodide by H_6**5c**$^{6+}$ [95] (Fig. 22) in a pseudotetrahedral geometry similar to that found for fluoride, except that in the latter one of the hydrogen bonds is between one water molecule and the fluoride anion.

Based in these data it is possible to conclude that the receptor cavity of H_n**5c**$^{n+}$ is too large to accommodate halide anions. Unfortunately, besides fluoride there are no reported association constants of H_n**5c**$^{n+}$ and other halide anions, making it impossible to establish a selectivity trend for the series of anions and to compare it with the respective macrocycle. In fact, association constants of the H_n**5c**$^{n+}$ with anions are scarce and discrepant values are found in the literature. Among the mononegative anions, only nitrate [52,89,96] and perchlorate have been studied [52]. The association constant between ClO_4^- and H_6**5c**$^{6+}$ was found to be 3.25 log units, and the respective crystal structure revealed the encapsulation of one perchlorate (Fig. 23) [52]. For nitrate, the association constant was also found to be higher for the cryptand than for the macrocycle (Table 17), and the crystal structure revealed two nitrate anions inside the cavity of the cryptand (Fig. 23), although there is no evidence that this is also found in solution, as the

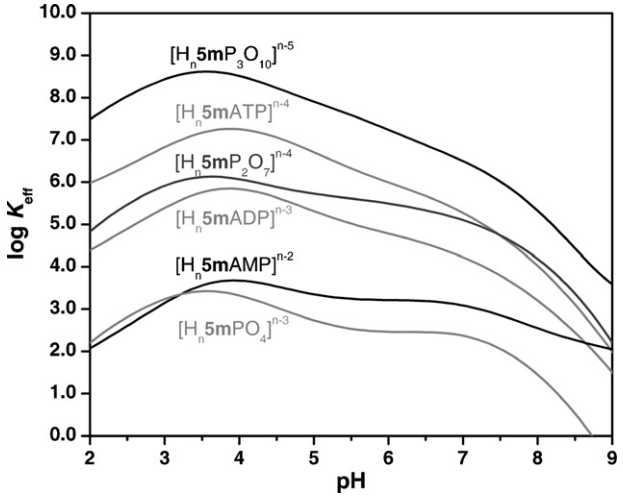

Fig. 21. Plots of the effective association constant ($\log K_{eff}$) *versus* pH for the entities formed by H_n**5m**$^{n+}$ with inorganic phosphates and nucleotide anions. I = 0.1 M KCl. $C_{\mathbf{5m}} = C_A = 2 \times 10^{-3}$ M.

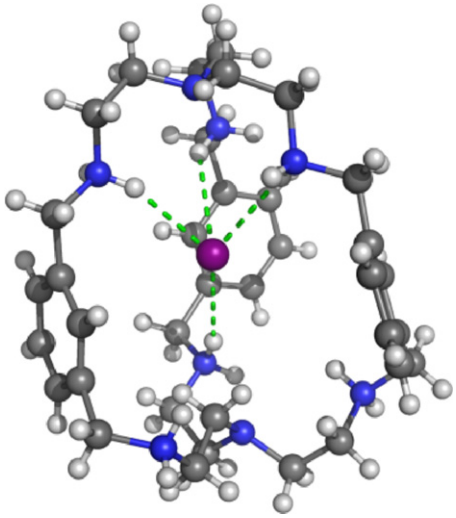

Fig. 22. X-ray crystal structure of the supermolecule formed by H_6**5c**$^{6+}$ with iodide [95].

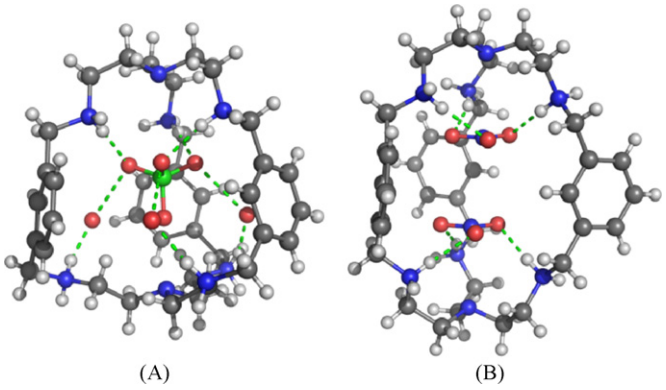

Fig. 23. Crystal structure of the supermolecule formed by $H_6\mathbf{5c}^{6+}$ with perchlorate (A) [52] and with nitrate (B) [89].

best model for fitting the potentiometric data indicated only the 1:1 receptor/substrate stoichiometry [89]. The enhanced affinity for nitrate and perchlorate anions by the cryptand relative to the macrocycle is due to the more appropriate spatial disposition of the binding sites in the cryptand allowing the encapsulation of these anions.

The sulfate binding is somewhat problematic as there are two different sets of association constant values with $H_n\mathbf{5c}^{n+}$, obtained in the same medium, reported by Bowman-James and coworkers [89] and Nelson and coworkers [85]. Bowman-James and coworkers have found almost no difference for the affinity of $H_6\mathbf{5m}^{6+}$ and $H_6\mathbf{5c}^{6+}$ for SO_4^{2-} [$\log K_{H_6\mathbf{5m}(SO_4)} = 4.36$ and $\log K_{H_6\mathbf{5c}(SO_4)} = 4.43$, see Table 17]. Curiously, the same result was found in pair 2 [$\log K_{H_6\mathbf{2m}(SO_4)} = 4.05$ and $\log K_{H_6\mathbf{2c}(SO_4)} = 4.20$] [35]. This means that the added dimensionality in $H_n\mathbf{5c}^{n+}$ relative to $H_n\mathbf{5m}^{n+}$ fails to enhance the affinity for sulfate as happens for NO_3^- and ClO_4^-, although the crystal structure of the association of SO_4^{2-} by $H_8\mathbf{5c}^{8+}$, which exists only in solution at very acidic pH, showed the sulfate encapsulated into the cavity of the receptor [97] (Fig. 24A). Therefore, these authors have not found any particular selectivity pattern between NO_3^-, ClO_4^- and SO_4^{2-} by $H_n\mathbf{5c}^{n+}$ [89]. On the other hand, Nelson and coworkers reported very high association constants for dinegative tetrahedral anions, such as SO_4^{2-}, SeO_4^{2-} and $S_2O_3^{2-}$ [9,85]. A log K value of 6.57 for the formation of $[H_6\mathbf{5c}SO_4]^{4+}$ was reported by these authors, a value much higher than that reported for $[H_6\mathbf{5m}SO_4]^{4+}$, see Table 17. Considering this value correct, one would conclude not only that the added dimensionality indeed increases affinity for sulfate by 2.21 log units relative to the macrocycle, but also that the cryptand is highly selective for sulfate over nitrate and perchlorate. Unfortunately, without additional experimental work, it is impossible to choose one of the values.

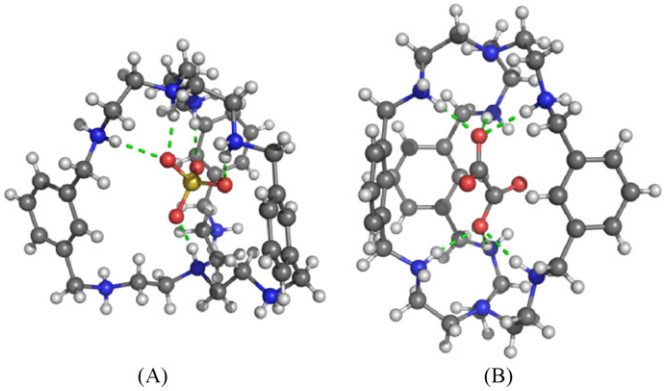

Fig. 24. Crystal structures of the supermolecules formed by $H_8\mathbf{5c}^{8+}$ with sulfate (A) [97], and of $H_6\mathbf{5c}^{6+}$ with oxalate (B) anions [87].

Nonetheless, it is odd that Bowman-James and coworkers found a heptaprotonated form of **5c** (not found in any other tren derived cryptand described in this review), and that it binds sulfate by only 0.54 log units stronger than does the hexaprotonated form. It is also unexpected that Nelson and coworkers found that the $H_6\mathbf{5c}^{6+}$ binds sulfate 1.85 log units stronger than the $H_5\mathbf{5c}^{5+}$ form does. The first difference seems to us too small and the second too large as, for instance, studies of $H_n\mathbf{2c}^{n+}$ with sulfate [35] revealed that $H_7\mathbf{2c}^{7+}$ binds sulfate 1.40 log units stronger than $H_6\mathbf{2c}^{6+}$ and $H_6\mathbf{2c}^{6+}$ binds the same anion 1.00 log units stronger than $H_5\mathbf{2c}^{5+}$.

Nelson and coworkers also studied the association of $H_n\mathbf{5c}^{n+}$ with carboxylate anions such as oxa^{2-}, mal^{2-}, ac^- and lac^- [9,48,87]. An extraordinary 4.88 log units enhancement of affinity towards oxalate by $H_6\mathbf{5c}^{6+}$ relative to $H_6\mathbf{5m}^{6+}$ was reported [9,85,87]. The unusually high association constant has been justified by the formation of six moderately strong hydrogen bonds with additional formation of π-stacking interactions between the C=O bond of one end of oxalate and two of the *m*-xylyl spacers of the cryptand (Fig. 24B). In this system the formation of $[H_7\mathbf{5c}oxa]^{5+}$ could be observed. The authors found it impossible to unambiguously assign the formation of this species to either $H_7\mathbf{5c}^{7+} + oxa^{2-}$ or $H_6\mathbf{5c}^{6+} + Hoxa^-$ reactions, however, because they never found $H_7\mathbf{5c}^{7+}$ in tosylate medium, they assigned that species for the purpose of calculation of a stepwise constant to $H_6\mathbf{5c}^{6+} + Hoxa^-$ and reported a $\log K_{H_7\mathbf{2c}(oxa)} = 13.83$ value. The authors pointed out that this value is anomalously large and concluded that some redistribution of the protons must occur during assembly, since in the pH range over which the species is formed neither $H_7\mathbf{5c}^{7+}$ nor oxa^{2-} are expected to be present in solution. If these values are correct this receptor is an excellent candidate to be used in analytical applications. However, these results are so high that need confirmation. Indeed, related receptors display much lower binding affinities, for instance $H_8\mathbf{2c}^{8+}$ binds oxalate 4.16 log units weaker than $H_6\mathbf{5c}^{6+}$ despite having two more positive charges [35], and $H_6\mathbf{4c}^{6+}$, being a very similar compound, also binds oxalate 2.41 log units weaker than $H_6\mathbf{5c}^{6+}$ [9,85,87].

3.6. *Macrocycle **6m** and cryptand **6c***

Unfortunately this pair of receptors, as well as the next one, has no binding studies with common anions reported. Therefore we briefly describe some features of each receptor.

The binding of $H_n\mathbf{6m}^{n+}$ with dicarboxylate anions, oxa^{2-} and od^{2-} [54] as well as phosphate derivatives, $P_3O_{10}^{5-}$ and ATP^{4-}

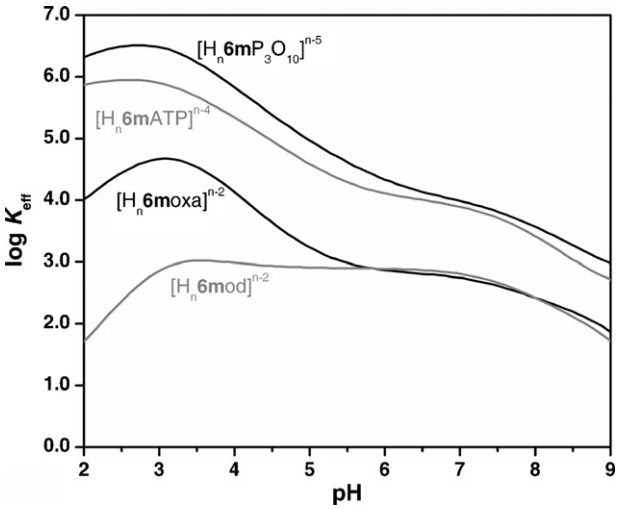

Fig. 25. Plots of log K_{eff} *versus* pH for the supramolecular species formed by $H_n\mathbf{6m}^{n+}$ with the indicated anions. $C_{\mathbf{6m}} = C_A = 2 \times 10^{-3}$ M [54,98].

Table 18
Stepwise association constants ($\log K_{H_hL_lA_a}$) for the indicated equilibrium in aqueous solution, T = 298.15 K.

Equilibrium[a]	$\log K_{L_lH_hA_a}$	
	L = **6m**	L = **6c**
$H_6L^{6+} + 2\ F^- \rightleftharpoons [H_6LF_2]^{4+}$	–	6.54[a]
$H_5L^{5+} + F^- \rightleftharpoons [H_5LF]^{4+}$	–	3.96[a]
$H_4L^{4+} + F^- \rightleftharpoons [H_4LF]^{3+}$	–	3.24[a]
$H_3L^{3+} + F^- \rightleftharpoons [H_3LF]^{2+}$	–	3.16[a]
$H_6L^{6+} + oxa^{2-} \rightleftharpoons [H_6Loxa]^{4+}$	6.08[b] (5.13*)	–
$H_5L^{5+} + oxa^{2-} \rightleftharpoons [H_5Loxa]^{3+}$	4.84[b] (4.03*)	–
$H_4L^{4+} + oxa^{2-} \rightleftharpoons [H_4Loxa]^{2+}$	2.82[b]	–
$H_3L^{3+} + oxa^{2-} \rightleftharpoons [H_3Loxa]^{+}$	2.32[b]	–
$H_2L^{2+} + oxa^{2-} \rightleftharpoons [H_2Loxa]$	2.22[b]	–
$H_6L^{6+} + Hod^- \rightleftharpoons [H_7Lod]^{5+}$	2.32[b]	–
$H_6L^{6+} + od^{2-} \rightleftharpoons [H_6Lod]^{4+}$	4.28[b] (3.39*)	–
$H_5L^{5+} + od^{2-} \rightleftharpoons [H_5Lod]^{3+}$	3.84[b] (3.09*)	–
$H_4L^{4+} + od^{2-} \rightleftharpoons [H_4Lod]^{2+}$	2.90[b]	–
$H_3L^{3+} + od^{2-} \rightleftharpoons [H_3Lod]^{+}$	2.30[b]	–
$H_2L^{2+} + od^{2-} \rightleftharpoons [H_2Lod]$	2.03[b]	–
$H_6L^{6+} + H_2P_3O_{10}^{3-} \rightleftharpoons [H_8LP_3O_{10}]^{3+}$	6.61[c]	–
$H_6L^{6+} + HP_3O_{10}^{4-} \rightleftharpoons [H_7LP_3O_{10}]^{2+}$	9.17[c] (6.67*)	–
$H_6L^{6+} + P_3O_{10}^{5-} \rightleftharpoons [H_6LP_3O_{10}]^{+}$	12.02[c] (4.68**)	–
$H_5L^{5+} + P_3O_{10}^{5-} \rightleftharpoons [H_5LP_3O_{10}]$	8.88[c] (4.04*)	–
$H_4L^{4+} + P_3O_{10}^{5-} \rightleftharpoons [H_4LP_3O_{10}]^{-}$	4.27[c] (3.75*)	–
$H_3L^{3+} + P_3O_{10}^{5-} \rightleftharpoons [H_3LP_3O_{10}]^{2-}$	3.66[c]	–
$H_2L^{2+} + P_3O_{10}^{5-} \rightleftharpoons [H_2LP_3O_{10}]^{3-}$	2.88[c]	–
$HL^{+} + P_3O_{10}^{5-} \rightleftharpoons [HLP_3O_{10}]^{4-}$	2.99[c]	–
$H_6L^{6+} + H_2ATP^{2-} \rightleftharpoons [H_8LATP]^{4+}$	6.01[c]	–
$H_6L^{6+} + HATP^{3-} \rightleftharpoons [H_7LATP]^{3+}$	7.05[c] (6.07*)	–
$H_6L^{6+} + ATP^{4-} \rightleftharpoons [H_6LATP]^{2+}$	9.83[c] (5.47**)	–
$H_5L^{5+} + ATP^{4-} \rightleftharpoons [H_5LATP]^{+}$	7.44[c] (4.06*)	–
$H_4L^{4+} + ATP^{4-} \rightleftharpoons [H_4LATP]$	3.97[c]	–
$H_3L^{3+} + ATP^{4-} \rightleftharpoons [H_3LATP]^{-}$	3.25[c]	–
$H_2L^{2+} + ATP^{4-} \rightleftharpoons [H_2LATP]^{2-}$	2.75[c]	–
$HL^{+} + ATP^{4-} \rightleftharpoons [HLATP]^{3-}$	2.61[c]	–

[a] I = 0.1 M in NaTsO, Ref. [56].
[b] I = 0.1 M in KCl, Ref. [54].
[c] I = 0.1 M in KCl, Ref. [98].
* Value in agreement with the K_{eff} *versus* pH diagram, indicating that the correct equilibrium was not ascribed by the authors; instead the correct one is established between the receptor having one less proton and one more in the anion.
** The correct equilibrium is established between the receptor having two less protons and the anion with two more protons.

[98] was reported. The association constants determined in aqueous solution by potentiometry (Table 18) show that H_n**6m**$^{n+}$ forms stable 1:1 supramolecular entities with these anions.

The effective constant values of H_n**6m**$^{n+}$ with dicarboxylate anions reach the maximum at pH ≈ 3 where coulombic interactions

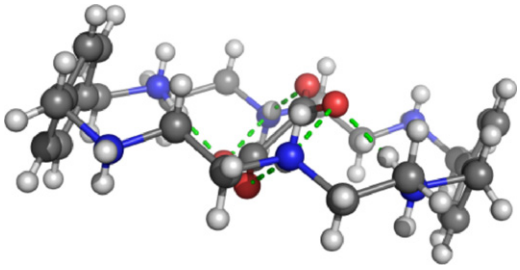

Fig. 27. Perspective view of the crystal structure of the association of H_6**6m**$^{6+}$ with oxa^{2-} [54].

and potential hydrogen bonds prevail, Fig. 25, log K_{eff} = 4.67 at pH 3.1 for the system H_n**6m**$^{n+}$:$H_n oxa^{n-2}$ and log K_{eff} = 3.02 at pH 3.6 for H_n**6m**$^{n+}$:$H_n od^{n-2}$.

The competitive diagram of the H_n**6m**$^{n+}$:$H_n oxa^{n-2}$:$H_n od^{n-2}$ system (Fig. 26) shows that H_n**6m**$^{n+}$ prefers the oxalate substrate at pH < 5.5, being at pH 2.0 selective for this anion. This feature was attributed to the rigidity of the anion and to the better accommodation of oxa^{2-} than od^{2-} into the macrocyclic cavity. The crystal structure of H_6**6m**$^{6+}$ with oxa^{2-} shows the oxalate located inside the cavity with two oxygen atoms directed upward and the other two downward in relation to the plane of the cavity. The anion is bound to the receptor through electrostatic interactions and weak to strong N^+–H···$^-$O hydrogen bonds (2.795–3.097 Å) involving only four secondary amines, Fig. 27 [54].

The evaluation of the binding ability of H_n**6m**$^{n+}$ as receptor for triphosphate and ATP (Table 18 and Fig. 25) [54] revealed the largest association constants for the formation of $[H_8$**6m**$P_3O_{10}]^{4+}$ and $[H_7$**6m**$P_3O_{10}]^{3+}$ (or $[H_8$**6m**$ATP]^{4+}$ and $[H_7$**6m**$ATP]^{3+}$), with log K_{eff} = 6.51 (or log K_{eff} = 5.94) at pH 2.8, where coulombic interactions and potential hydrogen bonds prevail. ^{1}H NMR experiments with 1:1 mixtures of free receptor and $P_3O_{10}^{5-}$ and ATP^{4-} substrates were also carried out at pH 4.5–5.9. The induced shift values provided evidence not only of the association of the substrates by the receptor but also of the existence of π–π interactions between the aromatic rings of the macrocycle and of the ATP^{4-} substrate. The competitive diagram, Fig. 26b for the H_n**6m**$^{n+}$/$H_nP_3O_{10}^{n-5}$/H_nATP^{n-4} system shows the preference of H_n**6m**$^{n+}$ for triphosphate over ATP at the entire pH scale.

The crystal structure $(H_6$**6m**$)Br_{1.33}(NO_3)_{4.66}\cdot 4H_2O$, showed the NO_3^- and Br^- anions located outside the cavity of the macrocycle (Fig. 28) [55]. The bromide anions are placed at each

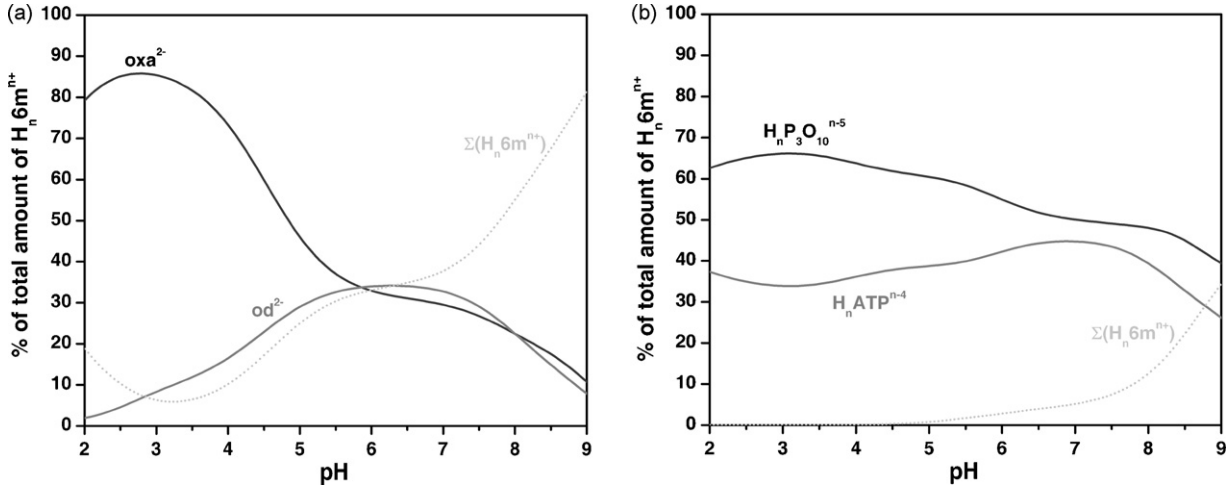

Fig. 26. Distribution diagram of the overall amount of supramolecular species formed between H_n**6m**$^{n+}$ and the mixture of $H_n oxa^{n-2}$ and $H_n od^{n-2}$ in 1:1:1 ratio (a); and the mixture of $H_nP_3O_{10}^{n-5}$ and H_nATP^{n-4} in 1:1:1 ratio (b). $C_{\mathbf{6m}} = C_A = 2 \times 10^{-3}$ M.

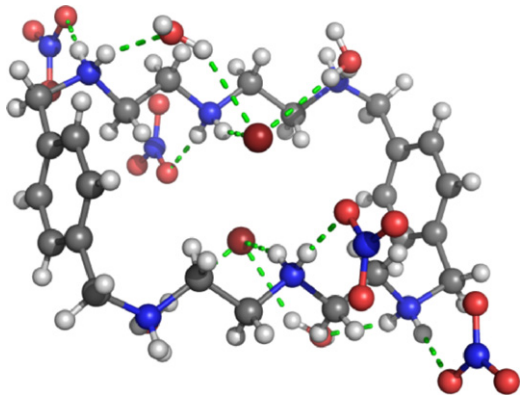

Fig. 28. Crystal structure $(H_6\mathbf{6m})Br_{1.33}(NO_3)_{4.66}\cdot 4H_2O$ [55].

side of the plane defined by the six nitrogen atoms at a distance of 1.75 Å. Nonetheless the authors considered this as quasi-encapsulation. A central ammonium group of the dien subunits and two water molecules (also connected to two terminal ammonium groups) hold bromide in place through hydrogen bonds.

Bowman-James and coworkers investigated the binding of $H_n\mathbf{6c}^{n+}$ with F^- [56], Cl^- and Br^- [99] anions, and the association constants, determined by ^1H NMR titrations in D_2O at pD 5, were 3.15, 3.37, and 3.34 (in log units) for F^-, Cl^-, and Br^-, respectively. The binding constants of F^- anion with $H_n\mathbf{6c}^{n+}$ were also determined by potentiometric methods, indicating that at pH 5 a mixture of penta- and hexaprotonated species are present in solution. The association constants increase as the pH decrease, and the formation of the $[H_6\mathbf{6m}F_2]^{4+}$ species was also found.

Crystal structures of the supramolecular entities formed by $H_6\mathbf{6c}^{6+}$ with the three anions were reported [56,99]. By a slight enlarge of the cavity size relative to $H_6\mathbf{5c}^{6+}$, $H_6\mathbf{6c}^{6+}$ uptakes two F^- anions and a bridged water molecule into its cavity, through $F^-\cdots H\text{–}O\text{–}H\cdots F^-$ hydrogen bonds, Fig. 29A. The supramolecular entity formed $[H_6\mathbf{6c}(F)_2(H_2O)][SiF_6]_2\cdot 12H_2O$ constitutes an anion-based cascade association, where two spherical anions play the topological role of the two metal ions in traditional cascade complexes. Each fluoride ion is located almost in the centre of the cavity, with the internal water molecule bridged somewhat to the outside. Each fluoride forms hydrogen bonds to three protonated secondary amines of one tren unit and the bridging water molecule in distorted tetrahedron geometry. The distances of the $N^+\text{–}H\cdots F^-$ hydrogen bonds fall into the range 2.60–2.72 Å, and the $F^-\cdots H\text{–}O\text{–}H$ distances are slightly longer of 2.71–2.72 Å. The isolation of an analogous structure in presence of Cl^- anions indicates that the fluoride cascade association is the preferred structure [56,99]. The other two structures $[H_6\mathbf{6c}(Cl)(H_2O)][Cl]_5\cdot 4H_2O\cdot CH_3OH$ and $[H_6\mathbf{6c}(Br)(H_2O)][Br]_5\cdot 6.25H_2O$, show a ditopic water/anion motif, and are quite similar to the structure of the fluoride binding by the related cryptand with *m*-xylyl spacers [99]. The halide anions are in a distorted tetrahedron geometry forming hydrogen bonds to three protonated secondary amines of one tren subunit and another one to the internal water molecule, Fig. 29B and C. Two more hydrogen bonds were detected between the internal water molecule and two secondary amines of the second tren unit. Also nitrate was found to bind to $H_6\mathbf{6c}^{6+}$ in a similar manner [8]. The formation of chloride/water and bromide/water entities rather than anion/water/anion entities, as happens for fluoride, is probably a reflection of the larger anionic radii for these anions, which makes the fit more favorable for just one halide in the cavity. Indeed iodide, being a larger halide, is found outside the cavity which in turn is occupied by three water molecules [100] (Fig. 29D). Interestingly, the structural features between the association of the three water molecules Fig. 29D and the anion cascade association of two fluorides and one water molecule depicted in Fig. 29A are quite similar. The distance between the bridgehead nitrogens in both structures is about the same and the distance between the two oxygen atoms of the two water molecules closer to the tren units in $[H_4\mathbf{6c}(H_2O)_4][I]_4\cdot 2.57H_2O$ and the distance between the two fluoride anions in $[H_6\mathbf{6c}(F)_2(H_2O)][SiF_6]_2\cdot 12H_2O$ have very close values (4.690 and 4.736 Å, respectively), with each water oxygen and fluoride almost equidistant from the bridgehead amines and each exhibiting pseudotetrahedral coordination *via* hydrogen-bonding interactions with the free/protonated amine hydrogens and bridging water molecules.

When the anion used as counter-ion is too large to fit the receptor cavity, invariably water molecules are found inside the receptor in the form of dimers (Fig. 30A), trimers (Figs. 29D and 30B and C) and even hexamers (Fig. 30D) [100,101]. The nature of the counter-ion [101], as well as the protonation state of the receptor [102,103], influences the shape and number of encapsulated water molecules, at least in the solid state. In our perspective, these structural studies illustrate well the fact that an anion needs not only to fit into the receptor cavity but also to be able to displace the water molecules that reside inside, which heavily compete with the anion for the binding sites, and of course also get rid of its own solvation water molecules. This is in agreement with the discussion in Section 3.1 of this review.

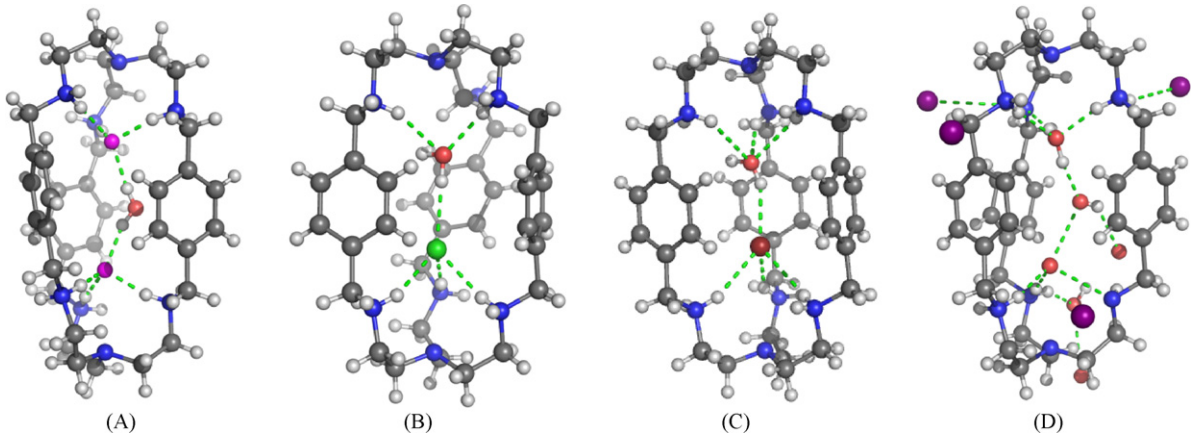

Fig. 29. Crystal structures of $[H_6\mathbf{6c}(F)_2(H_2O)][SiF_6]_2\cdot 12H_2O$ (A) [56], $[H_6\mathbf{6c}(Cl)(H_2O)][Cl]_5\cdot 4H_2OCH_3OH$ (B) [99], $[H_6\mathbf{6c}(Br)(H_2O)][Br]_5\cdot 6.25H_2O$ (C) [99] and $[H_4\mathbf{6c}(H_2O)_4][I]_4\cdot 2.57H_2O$ (D) [100].

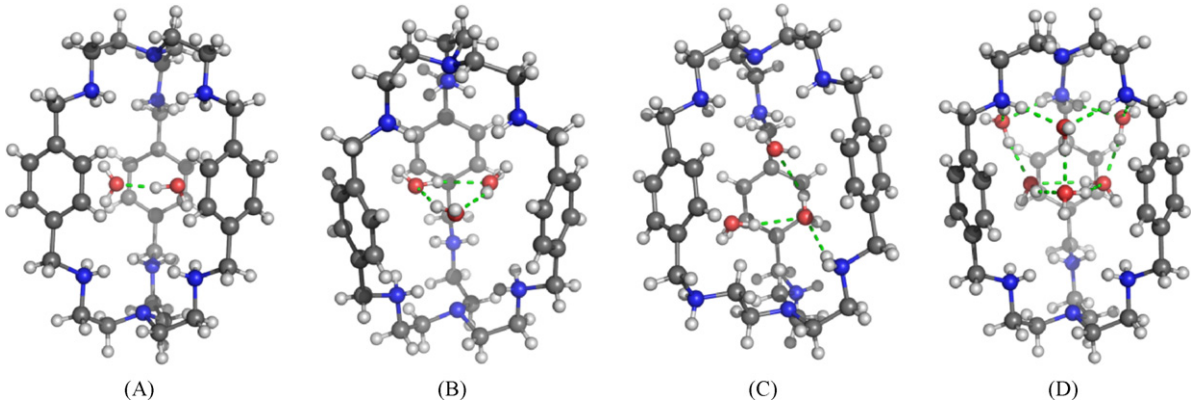

Fig. 30. Crystal structures of $[H_6\mathbf{6c}(H_2O)_2][H_2PO_4]_6{\cdot}3H_2O$ (A), $[H_6\mathbf{6c}(H_2O)_3][H_2PO_4]_6{\cdot}11H_2O$ (B), $[H_6\mathbf{6c}(H_2O)_3][TsO]_6{\cdot}4H_2O$ (C) and $[H_6\mathbf{6c}(H_2O)_6][SO_4]_3{\cdot}13H_2O$ (D) [101]. Counter ions omitted for clarity.

Curiously, and to remind us not to consider one crystal structure as the only conformation possible in solution, and that crystal structures must be seen with care, Ghosh and coworkers have found a binding motif in the associations of Cl^- and Br^- with $H_6\mathbf{6c}^{6+}$ [100] different from that presented in Fig. 29B and (C), in which only the anions occupy the receptor cavity and surprisingly there is no interaction between the protonated amines and the anions (Fig. 31). In another crystal structure, the association of chloride with the heptaprotonated form of **6c** [104] shows Cl^- interacting only with the protonated bridgehead amine and further stabilized inside the cavity not by the rest of the protonated amines but by three $(H_2O)_{11}$ clusters.

3.7. Macrocycle *7m* and cryptand *7c*

The association constants of $H_n\mathbf{7m}^{n+}$ with ADP and ATP were determined by potentiometric measurements by Martell and coworkers [44,57]. ATP is bound to $H_n\mathbf{7m}^{n+}$ more strongly than ADP and the differences between the log K_{eff} for ATP and ADP increase as the protonation degree on $H_n\mathbf{7m}^{n+}$ increases and reaches the maximum of 1.1 log units at pH 4.0. Curiously, $H_n\mathbf{7m}^{n+}$ binds ATP to a lesser extent than $H_n\mathbf{3m}^{n+}$, $H_n\mathbf{4m}^{n+}$ and $H_n\mathbf{5m}^{n+}$ (see Fig. 32), even though this macrocycle is very similar to the others. The authors could not find any explanation for this and suggested it may result from the different geometrical 'fit' of the substrate with respect to the receptor [57].

The rates of ATP-hydrolysis in the absence and presence of $H_n\mathbf{7m}^{n+}$ at pH 4.4 and 7.4 was also measured by HPLC [57]. It was found that at pH 4.4, the largest rate enhancement is promoted by $H_n\mathbf{7m}^{n+}$ compared with $H_n\mathbf{3m}^{n+}$, $H_n\mathbf{4m}^{n+}$ and $H_n\mathbf{5m}^{n+}$, in spite of its smaller K_{eff} value with ATP at pH 4.4, see Fig. 32. This means that besides strong association of the substrate by the catalyst, stabilization of the transition state is also necessary and, in this case, is accomplished by the availability of a good intramolecular nucleophile, the pyridyl nitrogen atom, which upon attack at the phosphorous centre of the nucleotide forms an intermediate phosphoramide and ADP. Since this type of intermediate could not be found with either $H_n\mathbf{4m}^{n+}$ or $H_n\mathbf{5m}^{n+}$ as catalysts, it was concluded that in these cases, the water molecule is the nucleophilic reagent [44,57].

Like for $H_n\mathbf{4c}^{n+}$ or $H_n\mathbf{5c}^{n+}$, the association of $H_n\mathbf{7c}^{n+}$ with dinegative tetrahedral anions such as SO_4^{2-}, SeO_4^{2-} and $S_2O_3^{2-}$ [9,85] and with carboxylate anions, such as oxa^{2-}, mal^{2-}, ac^- and lac^- [9,48] was studied by Nelson and coworkers [9,48,85]. The authors suggested, based on crystallographic data for the free cryptand [9] and its nitrate [9], perchlorate [105] and perrhenate [88] associations, that this receptor binds anions in a cleft manner rather than by encapsulation. This is apparently in agreement with the results obtained for the association with SO_4^{2-}, SeO_4^{2-} and $S_2O_3^{2-}$, where $H_6\mathbf{7c}^{6+}$ behaves as the weakest receptor compared with $H_6\mathbf{4c}^{6+}$ or $H_6\mathbf{5c}^{6+}$, but less sensitive to the deprotonation of receptor, in such a way that becomes the strongest receptor at higher pH values. The authors suggested that this tendency of the receptor to adopt cleft binding conformations and to be more geometrically adaptable also explains the very high association constants obtained for acetate, lactate and malonate, which surpass those obtained for $H_n\mathbf{4c}^{n+}$ and $H_n\mathbf{5c}^{n+}$ [9,48].

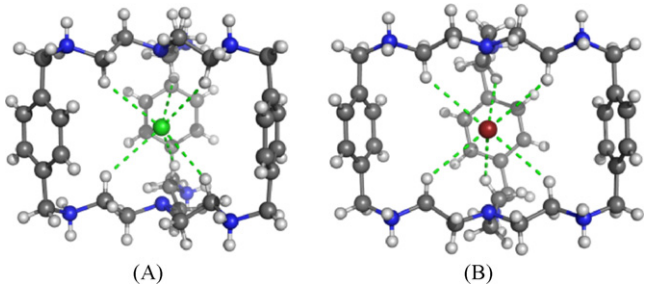

Fig. 31. Crystal structures of $[H_6\mathbf{6c}(Cl)][(Cl)_6H]{\cdot}10.86H_2O$ (A) and $[H_6\mathbf{6c}(Br)][(Br)_6H]{\cdot}4H_2O{\cdot}2HBr$ (B) [100].

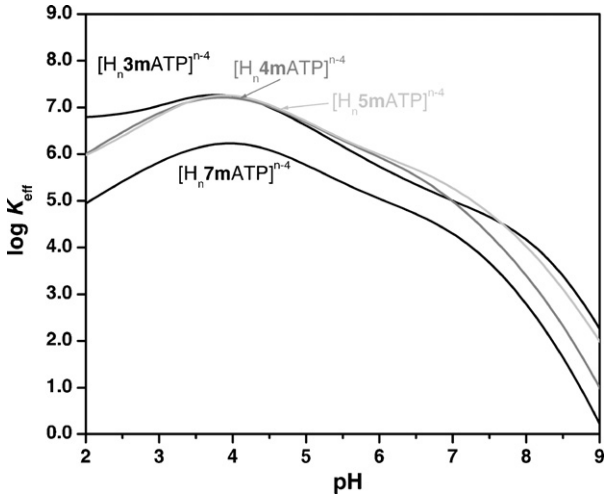

Fig. 32. Plots of the effective association constant (log K_{eff}) in function of the pH for the associations formed between $H_n\mathbf{3m}^{n+}$, $H_n\mathbf{4m}^{n+}$, $H_n\mathbf{5m}^{n+}$ and $H_n\mathbf{7m}^{n+}$ and H_iATP^{4-i}. $I = 0.1$ M KCl. $C_{receptors} = C_{ATP} = 2 \times 10^{-3}$ M.

Unfortunately there are no anions studied in common for H_n**7m**$^{n+}$ and H_n**7c**$^{n+}$ which prevents us from comparing these systems.

4. Conclusions

First we want to emphasize the importance of K_{eff} values as a very useful tool for the correct establishment of stepwise equilibria, especially when dealing with receptors and/or substrates with many and overlapping protonation states, as polyamines and polycarboxylates or polyphosphonates studied in water.

From the assessment of binding studies of seven polyammonium macrocycle/cryptand pairs as receptors for anions it is clear that electrostatic and hydrogen-bonding interactions provide the binding forces in anion association by these systems. Thus, in most cases the binding constants are explained on the basis of a simple electrostatic model, and then polyphosphate and nucleotides, especially ATP, present larger values, and polycharged oxoanions also exhibit larger association constants when compared with the monocharged anions. The exception is phosphate anion that can form many hydrogen bonds in which both the anion and the receptor act as acceptors or donors.

Thermodynamic functions of reactions were only reported for the H_n**1m**$^{n+}$ macrocycle, for which was possible to conclude that most of the reactions are accompanied by slightly unfavorable ΔH° contributions and largely favorable entropic terms, which is principally derived from desolvation of the interacting species determined by the charge neutralization occurring in the pairing process. Thus it seems that solvent release by both receptor and anion is an important driving force in these reactions. The cryptands, having a tri-dimensional cavity are likely to enclose more water molecules than the corresponding macrocycles and thus may benefit from more favorable entropic contributions upon solvent release. Of course that on the other side of the coin the enthalpic cost of desolvation should be higher than in the case of macrocycles. This may account for the fact that in general the binding constants of the cryptands are not much higher than those of the macrocycles. In fact, the added dimensionality of the cryptands results more in an increase of selectivity than in higher association constants. The selectivity may result from the complete displacement of the water molecules from the inside of the cryptand cavity by the anion that in turn requires the match of shape and size of the cryptand in order that the anion takes advantage of all the receptor binding sites. The encapsulation of one anion by the cryptand resulting in enhanced selectivity is clearly shown in the binding of oxalate and malonate by the H_n**3**$^{n+}$ and H_n**4**$^{n+}$ pairs, presented in Figs. 12 and 18. On the other hand, in general the macrocycle of each pair of receptors can bind a large variety of anions, although without any particular selectivity for series of substrates having the same number of identical functional groups. The results also indicate that the size, the geometry and the rigidity of the anion are very important features for the selective accommodation of the substrate into the cavity of the receptor. For instance, oxalate is in general preferred over the more flexible malonate.

It was also found that in general cryptands can better distribute the positive charges around the cavity allowing the repulsion between ammonium positive charges to be attenuated, resulting in complete protonation at pH about 6, with exception of the small **1c**. At this pH values most of the anions are completely deprotonated allowing a strong interaction. This represents an advantage of cryptands over macrocycles, which by contrast, are only completely protonated at pH about 4, except **2m** due to the propylenic chains separating the ammonium groups, allowing in most cases only stronger interactions with protonated forms of the anions, which are less charged and then decreasing the binding constant.

In conclusion, some general features derived from the dimensionality of the receptor and its effect on the binding of anions could be advanced based on the thermodynamics of the involved equilibria. It is likely that polyammonium macrocycles and cryptands will continue to inspire supramolecular chemists as they definitely stand out in the anion recognition field as fascinating receptors.

Colour code for atoms used in the crystal structures

The colour scheme used for atoms is gray for carbon, blue for nitrogen, white for hydrogen, red for oxygen, orange for phosphorous, yellow for sulfur, magenta for fluorine, green for chloride, dark red for bromine and purple for iodine. Hydrogen bonds are drawn as green dashed lines.

Abbreviations

Anions

ADP^{3-}	adenosine diphosphate
AMP^{2-}	adenosine monophosphate
ATP^{4-}	adenosine triphosphate
ac^-	acetate
ad^{2-}	adipate
btc^{3-}	1,3,5-benzenetricarboxylate
cit^{2-}	citrate
fum^{2-}	fumarate
glu^{2-}	glutarate
lac^-	lactate
$male^{2-}$	maleate
mal^{2-}	malonate
oxa^{2-}	oxalate
od^{2-}	oxydiacetate acid
sq^{2-}	squarate
suc^{2-}	succinate
tar^{2-}	tartrate
TsO^-	*p*-toluenesulfonate

Other

tren	*N*,*N*-bis(2-aminoethyl)-1,2-ethanediamine
trpn	*N*,*N*-bis(2-aminopropyl)-1,2-propanediamine

Acknowledgements

The authors thank the financial support from Fundação para a Ciência e a Tecnologia (FCT) with co-participation of the European Community funds FEDER, for the financial support under projects PTDC/QUI/56569/2004 and PTDC/QUI/68582/2006. Pedro Mateus acknowledge FCT for the grant, SFRH/BD/36159/2007 and Nicolas Bernier thanks ITQB for the grant 055/BI/2007. Authors thank S. Carvalho and V. Félix the help in obtaining cif files.

References

[1] P.A. Gale, 250, Coord. Chem. Rev. (2006) 2917.
[2] P.A. Gale, Coord. Chem. Rev. 240 (2003) 1.
[3] J.L. Sessler, P.I. Sansom, A. Andrievsky, V. Kral, in: A. Bianchi, K. Bowman-James, E. García-España, Pergamon (Eds.), Supramolecular Chemistry of Anions, Wiley-VCH, Oxford, NY, 1997, p. 355.
[4] F.P. Schmidtchen, Coord. Chem. Rev. 250 (2006) 2918.
[5] A. Bianchi, M. Micheloni, P. Paoletti, Coord. Chem. Rev. 110 (1991) 17.
[6] B. Dietrich, Pure Appl. Chem. 65 (1993) 1457.
[7] C.A. Ilioudis, J.W. Steed, J. Supramol. Chem. 1 (2001) 165.
[8] J.M. Llinares, D. Powell, K. Bowman-James, Coord. Chem. Rev. 240 (2003) 57.
[9] V. McKee, J. Nelson, R.M. Town, Chem. Soc. Rev. 32 (2003) 309.
[10] K. Bowman-James, Acc. Chem. Res. 38 (2005) 671.
[11] S. Kubik, C. Reyheller, S. Stüwe, J. Inclus. Phenom. Macrocycl. Chem. 52 (2005) 137.

[12] E. García-España, P. Díaz, J.M. Llinares, A. Bianchi, Coord. Chem. Rev. 250 (2006) 2952.
[13] K. Wichmann, B. Antonioli, T. Söhnel, M. Wenzel, K. Gloe, K. Gloe, J.R. Price, L.F. Lindoy, A.J. Blake, M. Schröder, Coord. Chem. Rev. 250 (2006) 2987.
[14] E.A. Katayev, Y.A. Ustynyuk, J.L. Sessler, Coord. Chem. Rev. 250 (2006) 3004.
[15] C. Cruz, R. Delgado, M.G.B. Drew, V. Félix, Org. Biomol. Chem. 2 (2004) 2911.
[16] F. Li, R. Delgado, V. Félix, Eur. J. Inorg. Chem. (2005) 4550.
[17] S. Carvalho, R. Delgado, N. Fonseca, V. Félix, New J. Chem. 1 (2006) 247.
[18] C. Cruz, R. Delgado, M.G.B. Drew, V. Félix, J. Org. Chem. 72 (2007) 4023.
[19] S. Carvalho, R. Delgado, M.G.B. Drew, V. Calisto, V. Félix, Tetrahedron 64 (2008) 5392.
[20] C. Cruz, V. Calisto, R. Delgado, V. Félix, Chem. Eur. J. 15 (2009) 3277.
[21] N. Bernier, S. Carvalho, F. Li, R. Delgado, M.G.B. Drew, V. Félix, J. Org. Chem. 74 (2009) 4819.
[22] P. Mateus, R. Delgado, P. Brandão, S. Carvalho, V. Félix, Org. Biomol. Chem. 7 (2009) 4661.
[23] P. Mateus, R. Delgado, P. Brandão, V. Félix, J. Org. Chem. 74 (2009) 8638.
[24] M.T. Albelda, M.A. Bernardo, E. García-España, M.L. Godino-Salido, S.V. Luis, M.J. Melo, F. Pina, C. Soriano, J. Chem. Soc., Perkin Trans. 2 (1999) 2545.
[25] A. Bianchi, E. Garcia-España, J. Chem. Ed. 76 (1999) 1727.
[26] A. Bencini, A. Bianchi, E. García-España, M. Micheloni, J.A. Ramirez, Coord. Chem. Rev. 188 (1999) 97.
[27] M. Kodama, E. Kimura, S. Yamaguchi, J. Chem. Soc., Dalton Trans. (1980) 2536.
[28] A. Bencini, A. Bianchi, M. Micheloni, P. Paoletti, E. Garcia-España, M.A. Niño, J. Chem. Soc., Dalton Trans. (1991) 1171.
[29] C. Bazzicalupi, A. Bencini, A. Bianchi, M. Cecchi, B. Escuder, V. Fusi, E. García-España, C. Giorgi, S.V. Luis, G. Maccagni, V. Marcelino, P. Paoletti, B. Valtancoli, J. Am. Chem. Soc. 121 (1999) 6807.
[30] J. Cullinane, R.I. Gelb, T.N. Margulis, L.J. Zompa, J. Am. Chem. Soc. 104 (1982) 3048.
[31] S.D. Reilly, G.R.K. Khalsa, D.K. Ford, J.R. Brainard, B.P. Hay, P.H. Smith, Inorg. Chem. 34 (1995) 569.
[32] B. Dietrich, B. Dilworth, J.-M. Lehn, J.-P. Souchez, M. Cesario, J. Guilhem, C. Pascard, Helv. Chim. Acta 79 (1996) 569.
[33] B. Dietrich, M.W. Hosseini, J.-M. Lehn, R.B. Sessions, J. Am. Chem. Soc. 103 (1981) 1282.
[34] B. Dietrich, M.W. Hosseini, J.-M. Lehn, R.B. Sessions, Helv. Chim. Acta 66 (1983) 1262.
[35] M.W. Hosseini, J.-M. Lehn, Helv. Chim. Acta 71 (1988) 749.
[36] J. Aragó, A. Bencini, A. Bianchi, E. García-España, M. Micheloni, P. Paoletti, A. Rodriguez, P. Paoli, Inorg. Chem. 30 (1991) 1843.
[37] S. Boudon, A. Decian, J. Fischer, W. Hosseini, J.-M. Lehn, G. Wipff, J. Coord. Chem. 23 (1991) 113.
[38] R.J. Motekaitis, A.E. Martell, J.-P. Lecomte, J.-M. Lehn, Inorg. Chem. 22 (1983) 609.
[39] A.E. Martell, R.J. Motekaitis, J. Am. Chem. Soc. 110 (1988) 8059.
[40] R.J. Motekaitis, A.E. Martell, Inorg. Chem. 30 (1991) 694.
[41] R.J. Motekaitis, A.E. Martell, Inorg. Chem. 31 (1992) 5534.
[42] P.E. Jurek, A.E. Martell, R.J. Motekaitis, R.D. Hancock, Inorg. Chem. 34 (1995) 1823.
[43] R.J. Motekaitis, A.E. Martell, Inorg. Chem. 33 (1994) 1032.
[44] A.E. Martell, R.J. Motekaitis, Q. Lu, D.A. Nation, Polyhedron 18 (1999) 3203.
[45] R.J. Motekaitis, A.E. Martell, J.-M. Lehn, E. Watanabe, Inorg. Chem. 21 (1982) 4253.
[46] B. Dietrich, J. Guilhem, J.-M. Lehn, C. Pascard, E. Sonveaux, Helv. Chim. Acta 67 (1984) 91.
[47] Q. Lu, R.J. Motekaitis, J.J. Reibenspies, A.E. Martell, Inorg. Chem. 34 (1995) 4958.
[48] J. Nelson, M. Nieuwenhuyzen, I. Pál, R.M. Town, Dalton Trans. (2004) 229.
[49] F. Arnaud-Neu, S. Fuangswasdi, B. Maubert, J. Nelson, V. McKee, Inorg. Chem. 39 (2000) 573.
[50] T.F. Pauwels, W. Lippens, P.W. Smet, G.G. Herman, A.M. Goeminne, Polyhedron 18 (1999) 1029.
[51] J.A. Aguilar, T. Clifford, A. Danby, J.M. Llinares, S. Mason, E. García-España, K. Bowman-James, Supramol. Chem. 13 (2001) 405.
[52] M.J. Hynes, B. Maubert, V. McKee, R.M. Town, J. Nelson, J. Chem. Soc., Dalton Trans. (2000) 2853.
[53] R. Menif, J. Reibenspies, A.E. Martell, Inorg. Chem. 30 (1991) 3454.
[54] C. Anda, A. Llobet, A.E. Martell, J. Reibenspies, E. Berni, X. Solans, Inorg. Chem. 43 (2004) 2793.
[55] M.G. Basallote, J. Durán, M.J. Fernández-Trujillo, M.A. Máñez, M. Quirós, J.M. Salas, Polyhedron 20 (2001) 297.
[56] M.A. Hossain, J.M. Llinares, S. Mason, P. Morehouse, D. Powell, K. Bowman-James, Angew. Chem. Int. Ed. 41 (2002) 2335.
[57] Q. Lu, R.I. Carroll, J.H. Reibenspies, A.E. Martell, A. Clearfield, J. Mol. Struct. 470 (1998) 121.
[58] R.I. Gelb, B.T. Lee, L.J. Zompa, J. Am. Chem. Soc. 107 (1985) 909.
[59] R.I. Gelb, L.B. Schwartz, L.J. Zompa, Inorg. Chem. 25 (1986) 1527.
[60] E. Kimura, A. Sakonaka, T. Yatsunami, M. Kodama, J. Am. Chem. Soc. 103 (1981) 3041.
[61] E. Kimura, A. Sakonaka, M. Kodama, J. Am. Chem. Soc. 104 (1982) 4984.
[62] E. Kimura, M. Kodama, T. Yatsunami, J. Am. Chem. Soc. 104 (1982) 3182.
[63] E. Kimura, A. Watanabe, M. Kodama, J. Am. Chem. Soc. 105 (1983) 2063.
[64] P. Arranz, A. Bencini, A. Bianchi, P. Diaz, E. García-España, C. Giorgi, S.V. Luis, M. Querol, B. Valtancoli, J. Chem. Soc., Perkin Trans. 2 (2001) 1765.
[65] A. Andrés, J. Aragó, A. Bencini, A. Bianchi, A. Domenech, V. Fusi, E. García-España, P. Paoletti, J.A. Ramírez, Inorg. Chem. 32 (1993) 3418.
[66] A.C. Warden, M. Warren, M.T.W. Hearn, L. Spiccia, New J. Chem. 28 (2004) 1301.
[67] A.C. Warden, M. Warren, M.T.W. Hearn, L. Spiccia, Inorg. Chem. 43 (2004) 6936.
[68] P.H. Smith, M.E. Barr, J.R. Brainard, D.K. Ford, H. Freiser, S. Muralidharan, S.D. Reilly, R.R. Ryan, L.A. Silks, W.-H. Yu, J. Org. Chem. 58 (1993) 7939.
[69] B. Dietrich, J.-M. Lehn, J. Guilhem, C. Pascard, Tetrahedron Lett. 30 (1989) 4125.
[70] Md.A. Hossain, J.M. Llinares, C.A. Miller, L. Seib, K. Bowman-James, Chem. Commun. (2000) 2269.
[71] M.A. Hossain, J.M. Llinares, N.W. Alcock, D. Powell, K. Bowman-James, J. Supramol. Chem. 2 (2002) 143.
[72] M. Arunachalam, E. Suresh, P. Ghosh, Tetrahedron 63 (2007) 11371.
[73] M.W. Hosseini, J.-M. Lehn, J. Am. Chem. Soc. 104 (1982) 3525.
[74] M.W. Hosseini, J.M. Lehn, Helv. Chim. Acta 69 (1986) 587.
[75] M.W. Hosseini, J.M. Lehn, Helv. Chim. Acta 70 (1987) 1312.
[76] M.R. da Silva, B. Szpoganicz, M. Lamotte, O.F.X. Donard, F. Fages, Inorg. Chim. Acta 236 (1995) 189.
[77] G. Papoyan, K.-j. Gu, J. Wiorkiewicz-Kuczera, K. Kuczera, K. Bowman-James, J. Am. Chem. Soc. 118 (1996) 1354.
[78] J.-M. Lehn, E. Sonveaux, A.K. Willard, J. Am. Chem. Soc. 100 (1978) 4914.
[79] R.J. Motekaitis, W.B. Utley, A.E. Martell, Inorg. Chim. Acta 212 (1993) 15.
[80] M.W. Hosseini, J.-M. Lehn, J. Chem. Soc., Chem. Commun. (1985) 1155.
[81] P.G. Yohannes, K.E. Plute, M.P. Mertes, K.B. Mertes, Inorg. Chem. 26 (1987) 1751.
[82] M.W. Hosseini, J.-M. Lehn, J. Chem. Soc., Chem. Commun. (1988) 397.
[83] Q. Lu, J.H. Reibenspies, R.I. Carroll, A.E. Martell, A. Clearfiled, Inorg. Chim. Acta 270 (1998) 207.
[84] Q. Lu, A.E. Martell, R.J. Motekaitis, Inorg. Chim. Acta 251 (1996) 365.
[85] J. Nelson, M. Nieuwenhuyzen, I. Pál, R.M. Town, Dalton Trans. (2004) 2303.
[86] B.M. Maubert, J. Nelson, V. McKee, R.M. Town, I. Pál, J. Chem. Soc., Dalton Trans. (2001) 1395.
[87] J. Nelson, M. Nieuwenhuyzen, I. Pál, R.M. Town, Chem. Commun. (2002) 2266.
[88] D. Farrell, K. Gloe, K. Gloe, G. Goretzki, V. McKee, J. Nelson, M. Nieuwenhuyzen, I. Pál, H. Stephan, R.M. Towna, K. Wichmann, Dalton Trans. (2003) 1961.
[89] T. Clifford, A. Danby, J.M. Llinares, S. Mason, N.W. Alcock, D. Powell, J.A. Aguilar, E. García-España, K. Bowman-James, Inorg. Chem. 40 (2001) 4710.
[90] M.G. Basallote, J. Durán, M.J. Fernández-Trujillo, M.A. Máñez, Polyhedron 20 (2001) 75.
[91] R. Menif, A.E. Martell, P.J. Squattrito, A. Clearfield, Inorg. Chem. 29 (1990) 4723.
[92] D.A. Nation, J. Reibenspies, A.E. Martell, Inorg. Chem. 35 (1996) 4597.
[93] D.A. Nation, Q. Lu, A.E. Martell, Inorg. Chim. Acta 263 (1997) 269.
[94] S. Mason, J.M. Llinares, M. Morton, T. Clifford, K. Bowman-James, J. Am. Chem. Soc. 122 (2000) 1814.
[95] I. Ravikumar, P.S. Lakshminarayanan, E. Suresh, P. Ghosh, Inorg. Chem. 47 (2008) 7992.
[96] S. Mason, T. Clifford, L. Seib, K. Kuczera, K. Bowman-James, J. Am. Chem. Soc. 120 (1998) 8899.
[97] S.O. Kang, M.A. Hossain, D. Powell, K. Bowman-James, Chem. Commun. (2005) 3228.
[98] C. Anda, M.A. Martínez, A. Llobet, Supramol. Chem. 17 (2005) 257.
[99] M.A. Hossain, P. Morehouse, D. Powell, K. Bowman-James, Inorg. Chem. 44 (2005) 2143.
[100] P.S. Lakshminarayanan, D.K. Kumar, P. Ghosh, Inorg. Chem. 44 (2005) 7540.
[101] Y. Li, L. Jiang, X.-L. Feng, T.-B. Lu, Cryst. Growth Des. 8 (2008) 3689.
[102] I. Ravikumar, P.S. Lakshminarayanan, E. Suresh, P. Ghosh, Cryst. Growth Des. 6 (2006) 2630.
[103] P.S. Lakshminarayanan, I. Ravikumar, E. Suresh, P. Ghosh, Cryst. Growth Des. 8 (2008) 2842.
[104] P.S. Lakshminarayanan, E. Suresh, P. Ghosh, Angew. Chem. Int. Ed. 45 (2006) 3807.
[105] V. McKee, G.G. Morgan, Acta Crystallogr. C 59 (2003) 150.